ECOSYSTEM RESPONSE TO HOLOCENE FIRE AND CLIMATE CHANGE AT HOBART LAKE, SOUTHWESTERN OREGON

by

Alicia Lauren White

A thesis submitted in partial fulfillment
of the requirements for the degree

of

Master of Science

in

Earth Sciences

MONTANA STATE UNIVERSITY
Bozeman, Montana

April 2014

ACKNOWLEDGEMENTS

I would like to thank my adviser Cathy Whitlock for her guidance, encouragement, and editing abilities that have helped me so much over the last few years. Thank you to my committee members Dave McWethy and Greg Pederson for their help throughout this entire process. I would like to thank Christy Briles for her advice, field and laboratory assistance, helpful responses to my innumerable email inquiries, and for her research that has been invaluable in conducting my own. I would also like to thank Caitlyn Florentine for her help with field and laboratory work, for introducing me to my entire social circle, and for always being my emotional cheerleader. Thank you to Virginia Iglesias, without whom I would not have survived statistics nor the steps required to complete this thesis. Her over-the-top willingness to help is much, much more appreciated than she knows. Thank you to Teresa Krause for answering my endless questions. She contributed greatly to the creation of figures in this thesis and my clarity of thought around many issues. Thank you to Laurie Stahle for being my battle buddy every step of the way. Her work ethic is astounding and I just attempted to keep her within sight. Thank you to Dave Firmage; his guidance at all stages of this process has been enormously helpful. Thank you to James Benes and Tim Turnquist for suddenly being the wonderful presence in the lab and my life that they are. Thank you to Gabe Yospin for all his help and advice. Thank you to James Mauch, Jeff Gay, and Paul Bodowski for all your work, the endless chats, and for always being a wonderful presence in the lab. Finally, thank you to my family for supporting me down my many paths over the years and always being a source of inspiration and support.

TABLE OF CONTENTS

1. ECOSYSTEM RESPONSE TO HOLOCENE FIRE AND CLIMATE CHANGE AT HOBART LAKE, SOUTHWESTERN OREGON....1

Contribution of Authors and Co-Authors....1
Manuscript Information Page....2
Introduction....3
Modern Setting....6
Methods....10
Lithological Analyses....11
Pollen....11
Charcoal....13
Results....15
Lithology....15
Chronology....17
Pollen and Charcoal....20
Discussion....24
Vegetation, Fire, and Climate History on the West Side of the Southern Cascade Range during the Last 8000 Years....25
History of *Abies* and *Pseudotsuga* in Oregon and Northern California....36
Conclusions....52

REFERENCES CITED....56

APPENDICES....63

APPENDIX A: Raw Charcoal Counts....64
APPENDIX B: Pollen Key....98
APPENDIX C: Raw Pollen Counts....101

LIST OF TABLES

Table Page

1. Radiocarbon and tephra dates used in age-depth model 18

2. Regional paleoecological sites referenced in the text 24

LIST OF FIGURES

Figure Page

1. Map of regional paleoecological sites and precipitation....4

2. Vegetation Zones of the southern Cascade Range....8

3. Lithologic, magnetic susceptibility, and LOI data for 2004 and 2011 cores....16

4. Age-depth model....19

5. Charcoal and pollen diagrams....22

6. Insolation, SSTs, and vegetation summaries from paleoecological sites....27

7. Sea-level pressure, surface winds, temperature, and precipitation for 16 ka, 14 ka, 11 ka, 6 ka, and present....28

8. CHAR, BCHAR, FRI, *Abies*, *Pseudotsuga*, Cupressaceae, insolation, and SSTs....32

9. *Abies* distribution map....38

10. *Pseudotsuga* distribution map....40

11. *Abies* pollen diagram....42

12. *Pseudotsuga* pollen diagram....47

ABSTRACT

Oregon's southern Cascade Range contains one of the world's most biologically diverse forests. Past ecosystem responses to fire and climate change have been well studied in the Coast Range, the eastern Cascade Range, and the Klamath Mountains but the ecological and environmental histories of the southern Cascade Range are poorly understood. Therefore, an 8000-year-long record from Hobart Lake (42.09935°N, 122.48170°W, 1458m), Oregon in the southern Cascade Range was examined to better understand past changes in vegetation and fire activity, conifer biogeographic distributions, and regional climate variability. Hobart Lake is exceptional in that it has an unusually fast sedimentation rate, resulting in a detailed vegetation and fire records based on pollen and macroscopic charcoal data. From 8000 to 3500 cal yr BP, the dominance of xerophytic species, such as *Pinus* and Cupressaceae, and the high frequency of fires are consistent with a climate that was warm and dry. Late-Holocene vegetation from 3500 cal yr BP to the present day was characterized by an abundance of mesophytic taxa, such as *Abies* and *Pseudotsuga*, and the decline of xerophytic taxa such as *Pinus*. These changes, along with reduced fire frequency, suggest that the climate became cooler and wetter. In addition to the Hobart Lake record, changes in the abundance of *Abies* and *Pseudotsuga* pollen at multiple sites throughout Oregon and northern California were examined. *Abies* was abundant during the late glacial, its range and/or abundance contracted during the early Holocene, and it gradually became more widespread and abundant during the mid- and late-Holocene. *Pseudotsuga* became more abundant at northern low-elevation sites during the warm dry conditions of the early Holocene and then flourished in more southern mid-elevation sites when the climate became cooler and wetter in the late Holocene. The vegetation history at Hobart Lake and other sites is consistent with large-scale variations in regional climate related to slowly varying changes in the seasonal insolation cycle and the indirect effects of insolation on the size and strength of the northeastern Pacific subtropical high-pressure system.

ECOSYSTEM RESPONSE TO HOLOCENE FIRE AND CLIMATE CHANGE AT HOBART LAKE, SOUTHWESTERN OREGON

Contribution of Authors and Co-Authors

Author: Alicia L. White

Contributions: Collected and analyzed data. Wrote all drafts of the manuscript.

Co-Author: Cathy Whitlock

Contributions: Conceived of study design and provided funding. Edited all drafts of the manuscript.

Co-Author: Christy E. Briles

Contributions: Conceived and implemented the study design. Provided field expertise and funding, and collected data. Edited a draft of the discussion.

Manuscript Information Page

Alicia L. White, Cathy Whitlock, Christy E. Briles
Quaternary Paleoecology
Status of Manuscript:
__x_ Prepared for submission to a peer-reviewed journal
____ Officially submitted to a peer-review journal
____ Accepted by a peer-reviewed journal
____ Published in a peer-reviewed journal

ECOSYSTEM RESPONSE TO HOLOCENE FIRE AND CLIMATE CHANGE AT HOBART LAKE, SOUTHWESTERN OREGON

Introduction

A key question in environmental sciences relates to how plant communities will respond to climate warming. The distribution of plant communities worldwide has shifted over millennial time scales and will likely shift in the future (*IPCC*, 2007). The analysis of paleoecological records provides information on the sensitivity of plant communities to a range of climate changes in the past as well as the role of natural disturbances. These insights are useful in evaluating ecosystem vulnerability to climate and land-management changes underway at present and projected for the future.

The mountainous region of northwestern California and southwestern Oregon is the junction between the southern Cascade Range, the northern Sierra Nevada, the Coastal Ranges, and the Klamath and Siskiyou Mountain ranges (*Western Ecology Division*, 2011). Elevations range from sea level to 2900 meters in a short distance, while steep gradients in altitude and precipitation create some of the sharpest climatic gradients in North America (*Franklin and Dyrness*, 1988; *Whittaker*, 1960). As a result of the climate, geology, and topography, northwestern California and southwestern Oregon support incredibly diverse vegetation with plant communities composed of species at the limits of their biogeographic ranges (*Odion and Sarr*, 2007; *U.S. Geological Survey*, 2006; *Whitlock et al.*, 2004; *Whittaker*, 1960; 1972).

Previous paleoecological studies in this region have focused on the fire, climate, and vegetation history of the Coast Range (*Worona and Whitlock*, 1995), the central and

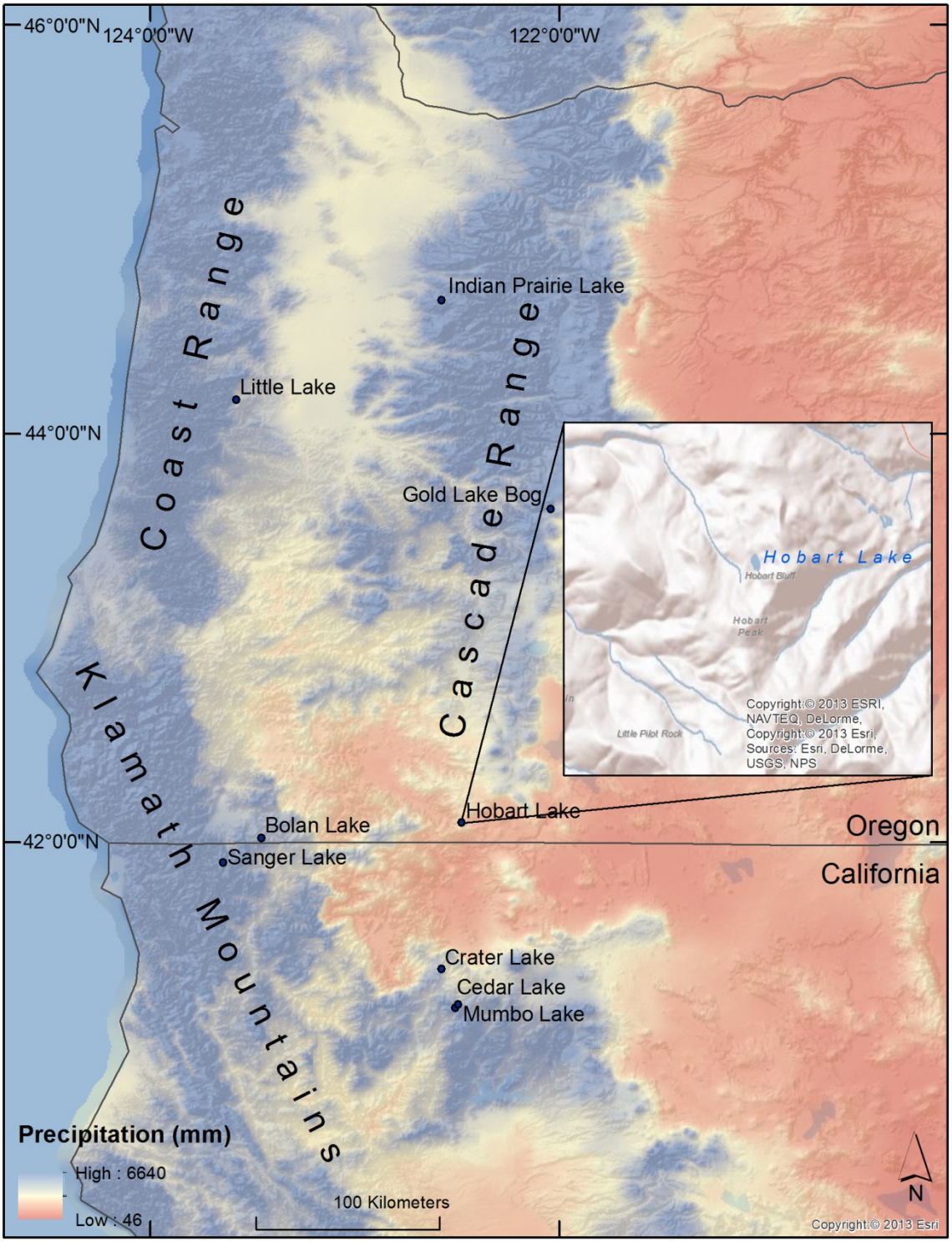

Figure 1. Hobart Lake and regional paleoecological sites with average annual precipitation from 1981-2010 (*PRISM Climate Group*, 2014).

eastern Cascade Range (*T Minckley et al.*, 2007; *Sea and Whitlock*, 1995), the Klamath and Siskiyou ranges (*Briles et al.*, 2005; *Daniels et al.*, 2005; *Mohr et al.*, 2000), and how substrate differences in the Klamaths influence vegetation and fire responses (*Briles et al.*, 2011) (Figure 1). Data from these studies show that vegetation and fire changes throughout the Holocene were strongly governed by large-scale variations in the climate system related to the seasonal cycle of insolation and its indirect effects, such as the expansion and intensification of the northeastern Pacific subtropical high-pressure system (*Bartlein et al.*, 1998). Records from the Klamath Mountains also display ecological responses to spatial differences in substrate that mute the response to past climate change (*Briles et al.*, 2011). No paleoecological information is available from the southern Cascade Range and this represents a gap in our understanding of how vegetation and fire regimes in this region, which is drier than the Coast, central Cascade, and Klamath ranges, have responded to Holocene variations in climate.

Accordingly, the main research objective of this study was to examine the vegetation, fire, and climate history on the west side of the southern Cascade Range. This was accomplished by reconstructing the vegetation and fire history of Hobart Lake (41.09935°N, 122.48170°W, 1458m, 3.2 hectares), based on an analysis of the pollen, charcoal, and lithologic contents of sediment cores (Figure 1). The record was then compared with paleoclimate model simulations to examine the vegetation and fire history with broad changes in climate over the Holocene (*Bartlein et al.*, 1998). The second objective of this study was to determine how *Abies* (fir) and *Pseudotsuga* (Douglas-fir), two of the dominant conifer genera in low- and middle-elevation forests in Oregon and

northern California, responded to changes in fire activity and climate over the past 16,000 cal years. This objective was addressed by comparing *Abies* and *Pseudotsuga* pollen records from Hobart Lake and other pollen sites in the Cascade Range, Coast Range, and Klamath Mountains (Figure 1) (*Briles et al.*, 2005; *Briles et al.*, 2011; *Daniels et al.*, 2005; *Mohr et al.*, 2000; *Sea and Whitlock*, 1995; *Worona and Whitlock*, 1995). This comparison provides information on past responses of two mid-elevation species to changes in fire and climate and provides a basis for anticipating how they may respond to future changes.

Modern Setting

Seasonal climate patterns at Hobart Lake are driven by shifts in high- and low-pressure systems in the northeastern Pacific Ocean (*Mock*, 1996). The expansion of the Aleutian Low in winter directs frontal storms and half of the yearly precipitation to this region (*Western Regional Climate Center*, 2013). The northeastern Pacific subtropical high-pressure system expands and intensifies in summer, which creates seasonally dry conditions. The present-day climate features cool wet winters and warm dry summers (*Skinner et al.*, 2006), although there is substantial variability due to significant altitudinal, and west-to-east and north-to-south temperature and precipitation gradients. An elevational temperature gradient exists from the coast to the Cascade crest, and the north-south-trending Coast and Cascade ranges intercept westerly storm tracks and create a steep west-to-east orographic precipitation gradient. At Hobart Lake, winter temperatures average 1.02°C, summer temperatures average 18.86°C, and annual temperatures average 8.70°C (*PRISM Climate Group*, 2014). Coastal areas near the

Oregon-California border receive up to 380 cm of rainfall per year, while areas just 80 km inland receive only 25-40 cm per year (*Daly et al.*, 2000). Precipitation at Hobart Lake averages 76 cm per year (*PRISM Climate Group*, 2014) with approximately 50% falling in the winter, and the remaining amount is divided evenly between the spring and fall seasons with very little precipitation received during the summer months (*Western Regional Climate Center*, 2013).

Hobart Lake is a landslide-dammed lake located in mixed-conifer forest dominated by *Pseudotsuga menziesii, Abies concolor* (white fir), and *Calocedrus decurrens* (incense cedar). The vegetation of the southern Cascade Range is arrayed along gradients of elevation and climate and also reflects changes in disturbance regimes (Figure 2) (*Odion and Sarr*, 2007). Hobart Lake lies in the *Abies concolor* zone, just above the mixed-conifer zone (*Franklin and Dyrness*, 1988). The watershed supports a closed forest of *Pseudotsuga menziesii*, *Abies concolor*, *Abies grandis* (grand fir), and *Calocedrus decurrens*. Although *Pinus lambertiana* (sugar pine) and *Pinus monticola* (western white pine) are characteristic of this zone, they are not found at Hobart Lake (*Franklin and Dyrness*, 1988). However, *Pinus ponderosa* (ponderosa pine) is abundant. Dry settings feature *Quercus garryana* (Oregon white oak) and to a lesser extent *Quercus kelloggii* (California black oak) and *Quercus brewerii* (Brewer's oak) (*The Nature Conservancy*, 1988). The understory of forests in the *Abies concolor* zone supports

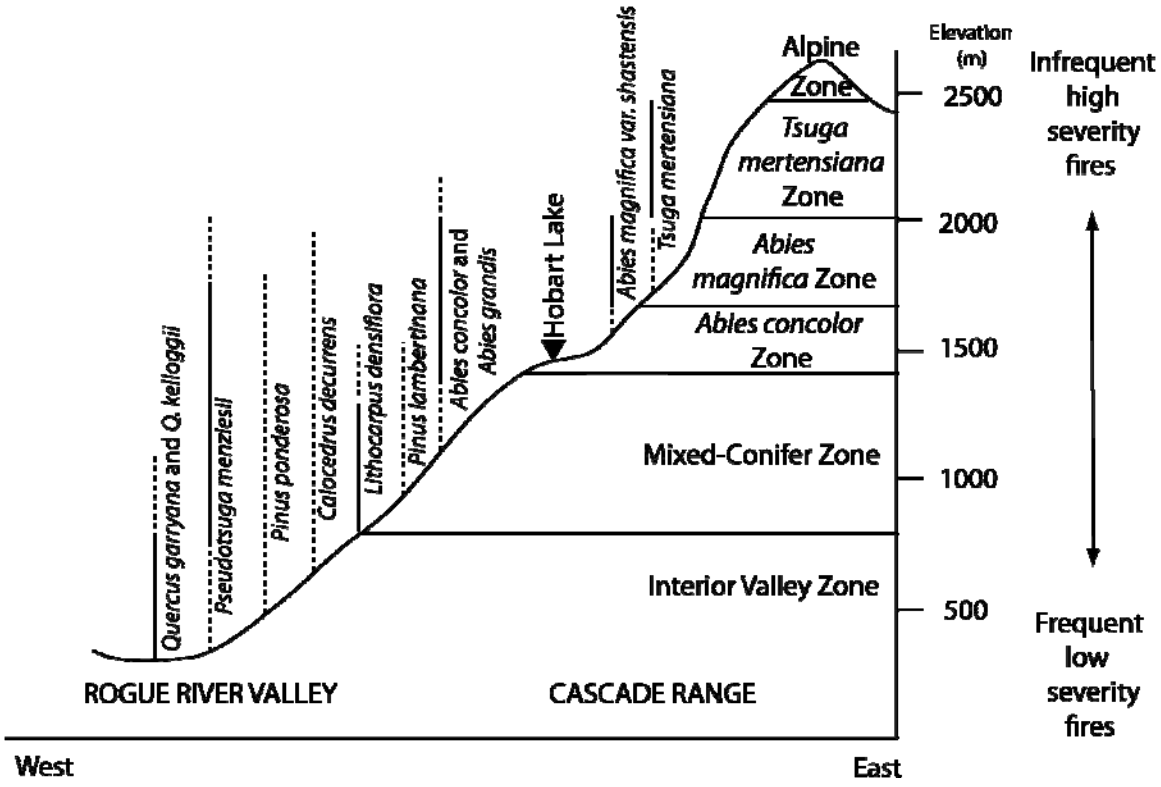

Figure 2. Modern vegetation zones and pre-European fire regimes of the southern Cascade Range. Solid vertical lines indicate elevations where the species is dominant and dashed lines indicate elevations where the species is present (based on Agee (1993), Briles et al. (2005) and Franklin and Dyrness (1988)).

a variety of shrubs, including *Holodiscus discolor* (ocean spray), *Rosa gymnocarpa* (baldhip rose), *Berberis nervosa* (dwarf Oregon-grape), *Corylus cornuta* var. *californica* (western beaked hazel), *Rubus ursinus* (California blackberry), *Rubus nivalis* (snow raspberry), *Acer glabrum* var. *douglassii* (vine maple), *Amelanchier alnifolia* (serviceberry), and *Castanopsis chrysophylla* (giant chinkapin) (*Franklin and Dyrness*, 1988). Common herbs in the *Abies concolor* zone include a variety of species in the Asteraceae, Apiaceae, Poaceae, Amaranthaceae, Polygonaceae, Brassicaceae, Urticaceae, Rosaceae, and Liliaceae families. Riparian areas surrounding the lake support *Acer*

macrophyllum (big-leaf maple), *Salix spp.*, *Cornus stolonifera* (red-osier dogwood), *Sambucus racemosa* (elderberry), and *Fraxinus latifolia* (Oregon ash). Aquatic species at Hobart Lake include *Nuphar lutea* (water lilies), *Lemna* (duckweed), *Myriophyllum* (watermilfoil), *Potamogeton* (pondweed*), Carex vesicaria* (blister sedge), *Carex obnupta* (slough sedge), *Typha latifolia* (cattail), and *Equisetum hyemale* (scouring rush) (*Guard*, 1995).

The Hobart Lake watershed has been shaped by a number of natural and human-caused disturbances in the past. It has been logged numerous times, transforming the forest from one predominantly of *Pseudotsuga menziesii*, *Abies concolor*, and *Calocedrus decurrens* forest to one composed largely of *Abies concolor* and *Pinus ponderosa*. More recently, *Picea breweriana* (Brewer's spruce), *Sequoiadendron giganteum* (sequoia), *Arbutus menziesii* (madrone), and *Pinus jeffreyi* (Jeffrey pine) have been cultivated by local landowners.

High temperatures, ongoing drought, above-average lightning occurrence, and a low snowpack in 2013 led to the most acres burned in this region in the last 50 years (*Oregon Department of Forestry*, 2013). Typically though, regional mixed-conifer and *Abies concolor* forests are characterized by low- to moderate-severity fire regimes (*Agee*, 1993). Natural ignitions through lightning occur more frequently in these forests than any other forest type in the Pacific Northwest, although Native Americans likely burned in the past to minimize undergrowth and maintain travel corridors, promote the growth of valuable species, and assist in promoting food sources and locating acorns in valley and foothill regions with *Notholithocarpus densiflorus* (tanoak) (*Agee*, 1993; *Lake*, 2013).

Native American burning is known to have occurred in the Willamette Valley and Cascade foothills, as well as on ridge tops to maintain travel corridors (*Agee*, 1993; *Walsh et al.*, 2010).

Methods

Two sets of 5-cm-diameter long cores were obtained from Hobart Lake with a modified Livingstone square-rod piston corer from a wooden platform across two inflatable kayaks anchored in the middle of the lake. The first core, measuring 11.47 m long, was obtained in 2004 by Christy Briles, and the second, measuring 10.01 m in length, was recovered in 2011 by Christy Briles, Ali White, and Caitlyn Florentine of Montana State University (MSU), and Scott Starratt, Elmira Wan, Jenn Kusler, and Holly Olson of the US Geological Survey (USGS). Both sets of long cores were extruded, visually examined and briefly described on site. They were packaged in plastic wrap, aluminum foil, and placed in core boxes for safe transport to the MSU Paleoecology Lab where they were refrigerated.

In the laboratory, both cores were split longitudinally, described, and photographed. One-third of the 2011 core was archived. The top two meters of the 2004 core dried significantly between 2004 and 2011, and the stratigraphy was judged to be unreliable. No further analysis was conducted on the 2004 core between 0 and 2.00 meters depth. The 2011 core was obtained to fill in this missing upper section. It was correlated with the 2004 core based on shared litho- and chronostratigraphy (see results).

Therefore, the top 2.35 m of the 2011 core and the bottom 9.17 meters of the 2004 core were used for all analysis and treated as a single record.

Lithological Analyses

Loss on ignition (LOI) was undertaken to quantify organic and carbonate content of the lake sediment, which is used as a proxy for lake productivity, and was conducted at 5-cm intervals (*Dean Jr.*, 1974). For each interval, 1-cm^3 of sediment was heated at 80°C for 24 hours to dry the material. The sediment was then placed in a furnace and heated to 550°C for 2 hours to remove organic material. The samples were then heated to 900°C for an additional 2 hours to remove the inorganic carbonates. Sample weights were obtained between each procedural step. Magnetic susceptibility was measured with a Bartington magnetic susceptibility core logging sensor. Meter-long core segments were run through the logging sensor and measurements were taken at 0.5-cm increments (*Dearing*, 1999). Peaks in magnetic susceptibility, expressed in CGS x 10^{-6} units, record the input of ferromagnetic minerals from allochthonous material. These peaks are an indication of erosional and fire events (*Gedye et al.*, 2000). Magnetic susceptibility was completed for the entire 2011 core and portions of the 2004 core containing tephra layers to assist in core correlation (Figure 3).

Pollen

Pollen analysis was undertaken to reconstruct the vegetation history. Sediment samples of 1 cm^3 volume were extracted from the entire length of the core at 16-cm intervals and processed to isolate the pollen using the methods described in Bennett and

Willis (2001). *Lycopodium* spore tablets of a known concentration were added during pollen processing. Based on the age-depth model, this sampling interval represents about one sample every 107 years. The resulting pollen was mounted in silicone oil on slides and observed under a microscope at 400x magnification. Reference slides and pollen identification keys (*Faegri and Iversen*, 1975; *Kapp et al.*, 2000; *McAndrews et al.*, 1973) were consulted to identify each pollen grain to the lowest taxonomic level possible. A minimum of 300 terrestrial pollen grains was counted for each slide. Pollen percentages were calculated as a percent of total counted terrestrial pollen. Aquatic pollen percentages were calculated as a percentage of total terrestrial and aquatic pollen. This information was plotted using C2 and Tilia software, with zone designation conducted using CONISS cluster analysis techniques in Tilia (*Grimm*, 1987).

Pollen accumulation rates (grains cm^{-2} yr^{-1}) were calculated by dividing pollen concentration by the deposition time. Pollen concentration was calculated by dividing the number of terrestrial pollen grains by the number of L*ycopodium* spores counted; this value was divided by the total *Lycopodium* concentration of the sample (13,911). Deposition time was calculated as the difference in age between each successive sample divided by the depth interval.

Pinus pollen counts include Haploxylon-type, Diploxylon-type and undifferentiated *Pinus* grains. The Haploxylon-type pines were attributed to *Pinus lambertiana* (sugar pine) and the Diploxylon-type are to *Pinus ponderosa* (ponderosa pine) on the reasoning that both species grow in the watershed at present. Diploxylon-type *Pinus* may also come from *P. contorta* (lodgepole pine), which presently grows 20

km east of Hobart Lake. *Abies* pollen was assigned to *Abies grandis* and *Abies concolor*. *Quercus* pollen types, distinguished by their sculpture, include deciduous *Quercus garryana* and evergreen *Quercus vaccinifolia* (huckleberry oak). Rosaceae pollen included *Spiraea*, *Amelanchier*, and *Potentilla*. Total arboreal pollen taxa included *Pinus*, *Abies*, *Pseudotsuga*, Cupressaceae, *Alnus rubra*-type, *Alnus sinuata*-type, *Corylus*, *Salix*, *Populus*, *Fraxinus*, *Quercus vaccinifolia*-type, *Quercus garryana*-type, *Acer macrophyllum*, *Acer circinatum*, Rosaceae, *Ceanothus*, *Chyrsolepis/Lithocarpus*, *Arceuthobium*, *Cornus*, *Cercocarpus*, and *Sarcobatus*. Nonarboreal pollen taxa included Poaceae, *Artemisia*, Asteraceae *Tubuliflorae*, Asteraceae *Liguliflorae*, Amaranthaceae, Apiaceae, *Polygonum californicum*-type, Brassicaceae, *Urtica*, Liliaceae, and Lamiaceae. Pollen grains that were unidentifiable were counted as 'Unknown' while those that were degraded, damaged, or hidden were counted as 'Indeterminate.'

Charcoal

Macroscopic charcoal analysis was conducted to reconstruct the local fire history near Hobart Lake. Samples of 2 cm^3 were taken at 1-cm intervals in the 2004 and 2011 cores. Each of the 1240 samples was placed in a solution of 10% sodium hexametaphosphate ($(NaPO_3)_6$) and 8.25% bleach (NaClO). $(NaPO_3)_6$ is a diffloculant used to dissipate clay particles, and the bleach solution oxidizes non-charcoal organic material, which facilitates charcoal identification. After the samples were soaked in this mixture for 24 hours, they were gently rinsed through a 125-µm mesh sieve, and the residue was transferred to a gridded petri dish. This 125-µm mesh size was selected because previous studies have shown that particles larger than this size capture a local

fire signal as charcoal particles are too heavy to be transported long distances (*Whitlock and Larsen*, 2001). All charcoal fragments in a petri dish were then tallied under a stereoscope. Where possible, grass charcoal was morphologically differentiated from wood charcoal to determine their relative proportion.

Statistical analysis of the charcoal data was conducted using the CHARAnalysis program (https://sites.google.com/site/charanalysis/) and the methods described in Higuera et al. (2009) were used to reconstruct the local fire history of Hobart Lake. CHARAnalysis converted charcoal count data into charcoal accumulation rates (CHAR), measured in particles $cm^{-2}\ yr^{-1}$. This information was continuously resampled in 8-year bins, which is the median sample resolution of the Hobart Lake record, to account for sedimentation rate changes. CHARAnalysis is designed to differentiate the slowing varying component of the charcoal time series (so-called background charcoal or BCHAR) from high-frequency deviations or charcoal peaks that indicate individual fire episodes. BCHAR was inferred to come from regional fire activity and biomass burning while the positive residuals of the model (i.e. charcoal peaks) denote local fire events as well as noise (*Higuera et al.*, 2009; *Whitlock and Anderson*, 2003). Fire episodes and fire return intervals were inferred from the peak component. The background charcoal trend was established using a 600-year lowess smoother considered an ideal fit to the data because it balanced the signal-to-noise index and the noise distribution goodness of fit. The signal-to-noise index indicates how much variation in charcoal values is likely to be significant (i.e. a fire episode) versus random noise. The noise distribution goodness of fit is a measure of how well the background charcoal levels fit the charcoal accumulation

rate data. Charcoal peaks were established by subtracting background charcoal levels from the charcoal accumulation rate at particular stratigraphic level. A locally-defined threshold using a Gaussian mixture model was applied to the charcoal peak data to determine the noise distribution. Values above the 95th percentile were designated as fire episodes. A Poisson distribution was applied to the fire-episode data and multiple peaks within a single distribution were eliminated as they likely came from a single fire event. Fire-episode frequencies were then smoothed with a 1000-year window.

Results

Lithology

The 2004 and 2011 Hobart Lake sediment cores were composed primarily of fine-detritus gyttja (Figure 3). The bottom of the 2004 core from 11.47 to 8.30 m depth (Unit 1) contained dark fine-detritus gyttja interspersed with inorganic clay and coarse sand layers, ranging in thickness from 1 to 3 cm. The inorganic sediments likely reached the lake through a series of erosional events. Unit 2 (8.30 to 5.20 m depth) contained banded fine-detritus gyttja. Above 5.20 m depth (Unit 3), the gyttja was largely homogenous implying a fairly closed and productive lake environment. Unit 1 had the highest and most variable magnetic susceptibility values (ranging from 0 to 510 CGS x 10^{-6}) and relatively low organic content values. A tephra layer was identified at 10.90 m depth. Based on the age model, this tephra was inferred to be the Mazama ash, which erupted at 7627 ± 150 cal yr BP (*Zdanowicz et al.*, 1999). Above the Mazama ash, the core

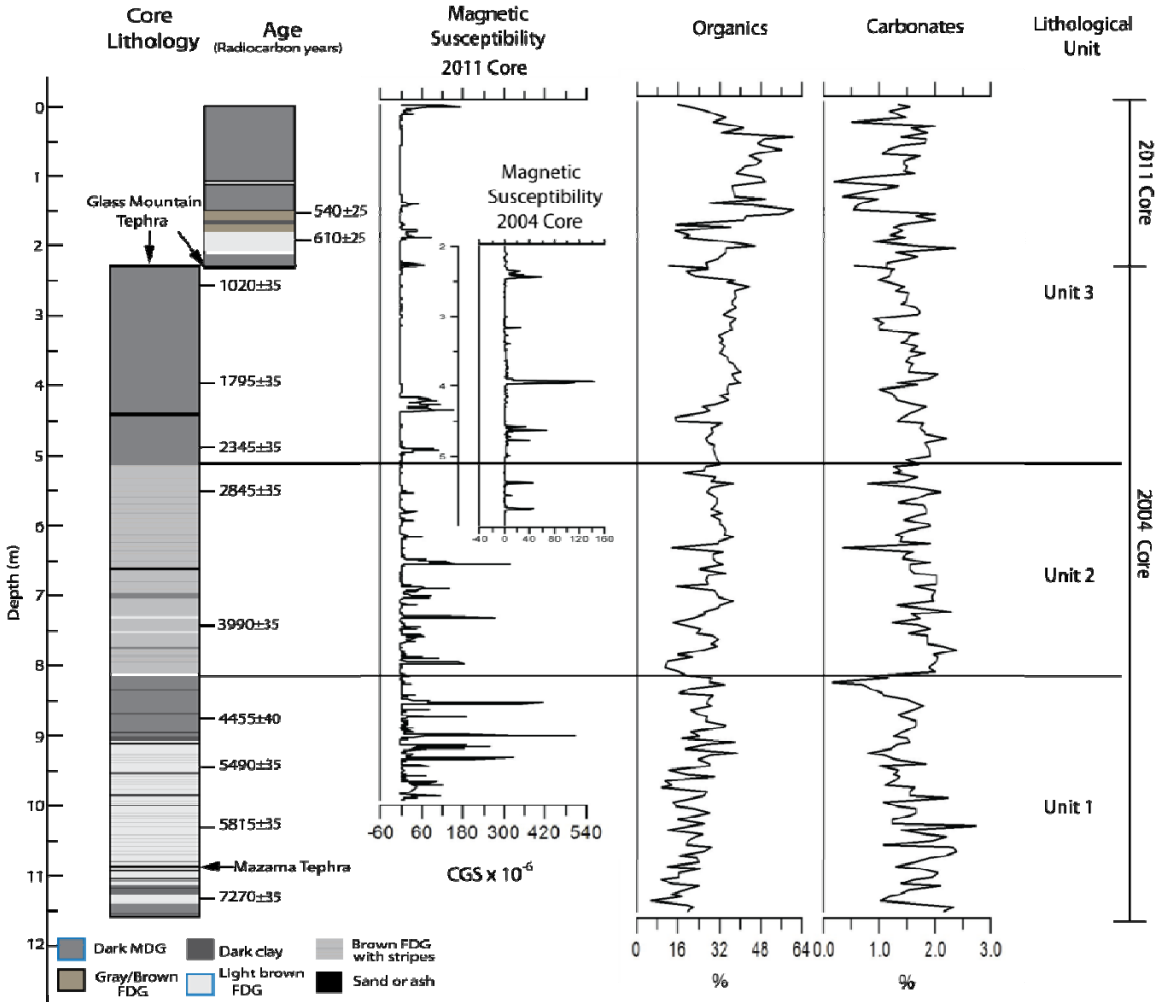

Figure 3. Lithology, radiocarbon dates, magnetic susceptibility data, and percent organic and inorganic content for the 2004 and 2011 Hobart Lake cores. FDG stands for fine-detritus gyttja and MDG stands for medium-detritus gyttja.

consisted of several meters of light-colored fine-detritus gyttja with coarsely banded clay layers that were especially abundant from 8.30 to 9.00 m depth. Magnetic susceptibility values varied widely in this section from values of 0 to 412 CGS x 10^{-6}. In Unit 2 (8.30 to 5.00 m depth), the core contained banded light and dark fine-detritus gyttja with a transition to primarily dark fine-detritus gyttja above 5 m depth. There was a likely ash

layer from 4.34 to 4.35 m depth, the source was unidentified. Peaks in the magnetic susceptibility data occurred at this depth as well, with values as high as 155 CGS x 10^{-6}. The top of the 2004 core to the correlation point with the 2011 core at 2.30 m depth contained dark medium-detritus gyttja with increasing plant remains. A tephra layer at 2.30 m depth was identified as Glass Mountain tephra, based on tephra samples submitted to a tephrachronology lab, which have a known age of 890-940 cal yr BP (Elmira Wan, USGS, personal communication).

Overlying the same tephra layer in the 2011 core was fine-detritus gyttja with a light brown layer occurring at 2.10 m depth. A gray-brown layer occurred from 1.92 to 1.64 m depth with a dark clay band from 1.73 to 1.75 m depth. The top 1.50 m of the 2011 core contained homogenous dark medium-detritus gyttja with noticeable quantities of plant detritus. Small spikes in the magnetic susceptibility values up to 161 CGS x 10^{-6} occurred in this portion of the core along with the highest organic content values found throughout the 2004 and 2011 cores. In summary, occasional erosional events delivered pulses of inorganic sediment to Hobart Lake in the early record, whereas autochthonous sediment characterized deposition in more recent sediments. The difference in lithology reflects either a decrease in extreme weather events and/or increasing forest cover in the watershed through time.

Chronology

Plant macrofossils from eleven levels in the 2004 core and three levels from the 2011 core were submitted for AMS radiocarbon dating, and the results were used to create an age-depth model (Table 1 and Figure 4). The point of correlation on the cores

Table 1. Age information used to construct the chronology for Hobart Lake.

Depth (cm)[a]	Core	Uncalibrated ^{14}C age (^{14}C yr BP)	±	Calibrated age (cal yr BP) with 2-sigma range[b]	Material Dated	Lab Number[c]
153	Hobart 2011B	540	25	508 - 550	Seed	OS-98623
192	Hobart 2011B	610	25	577 - 653	Twig	OS-98622
241	Hobart 2011B	1080	25	934 - 1014	Wood	OS-98621[d]
235	Hobart 2011B	na	na	890 - 940	Glass Mountain Tephra	
230	Hobart 2004B	na	na	890 - 940	Glass Mountain Tephra	
63	Hobart 2004B	155	30	166 - 231	Peat	118785[d]
167	Hobart 2004B	510	30	505 - 555	Peat	119600[d]
244	Hobart 2004B	1020	35	900 - 988	Wood	119601
379	Hobart 2004B	1795	35	1686 - 1821	Grass	119602
475	Hobart 2004B	2345	35	2311 - 2473	Twig	119603
545	Hobart 2004B	2845	35	2866 - 3068	Wood	119604
736	Hobart 2004B	3990	35	4405 - 4534	Wood	119605
861	Hobart 2004B	4455	40	4959 - 5148	Wood	119606
935	Hobart 2004B	5490	35	6263 - 6324	Wood	119607
1017	Hobart 2004B	5815	35	6501 - 6679	Twig	119608
1128	Hobart 2004B	7270	35	8012 - 8169	Wood	119609

[a] Depth below mud surface
[b] Ages calibrated with CALIB 6.0
[c] National Ocean Sciences AMS Facility, Woods Hole Oceanographic Institute
[d] Date not used in age-depth model.

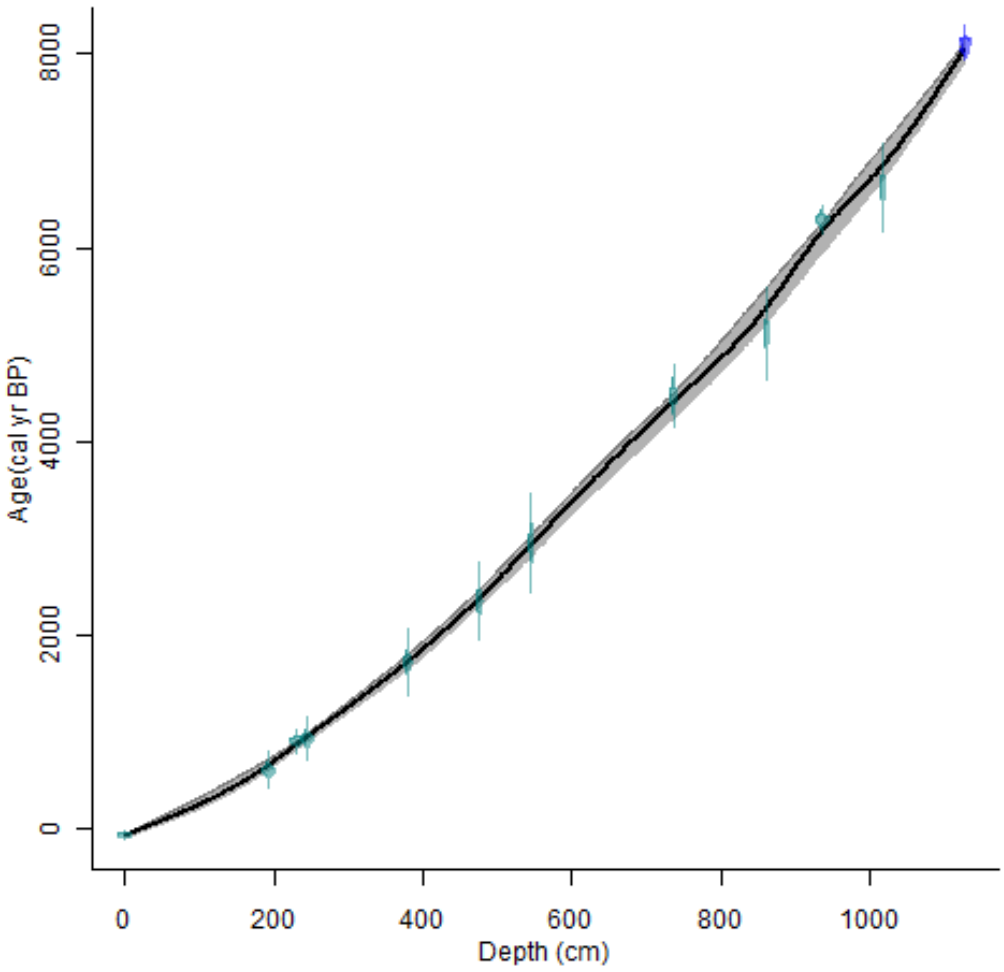

Figure 4. Age-depth curve for Hobart Lake. The black line indicates the interpolated age at each depth. The gray bar is a 95% confidence interval surrounding the age-depth curve. Radiocarbon and tephra dates are depicted as small circles with vertical error bars. Clam 2.1 (http://chrono.qub.ac.uk/blaauw/clam.html) was used within R (http://www.r-project.org/) to create the age-depth curve.

was drawn at 2.20 m depth on the 2011 core and 2.30 m depth on the 2004 core.

Radiocarbon dates younger than the Glass Mountain tephra in the 2011 core and older than tephra in the 2004 core were not included in the age-depth model. A tephra layer at

14.90 m depth in the 2004 core, inferred to be Mazama ash, was included in the age model.

Radiocarbon dates were calibrated using CALIB 6.0 (*Reimer et al.*, 2009; *Stuiver et al.*, 2010), and Clam 2.1 software (http://chrono.qub.ac.uk/blaauw/clam.html) was used within R (http://www.r-project.org/) to create the age-depth curve. A smoothing spline set to 0.3 was used, in which 0 means no smoothing and 1 is a straight line. The 95% confidence intervals for the curve were calculated by repeated sampling of the individual radiocarbon and tephra date confidence intervals (*Blaauw*, 2010). Random points were selected within each date's confidence interval and a line was drawn connecting the points. This sampling procedure was repeated 1000 times to develop the confidence interval for the age-depth model.

Pollen and Charcoal

The pollen record was divided into three zones based on CONISS cluster analysis (Figure 5) (*Grimm*, 1987). Zone HL-1 (11.34-9.54 m depth; ca. 7930-6300 cal yr BP) had high percentages of *Pinus* (41-76%), with 2.5-17.5% of the record composed of Haploxylon-type *Pinus* and 0.3-4.4% of Diploxylon-type *Pinus*. *Abies* (0.3-6%) and *Pseudotsuga* (0.3-5%) values were low, whereas Cupressaceae percentages (7-29%) were the highest of the record. *Alnus rubra*-type pollen was found in low percentages in this zone, representing between 0-3% of the record. *Salix* percentages ranged from 0.3% to 1.6%. Deciduous-type *Quercus* comprised a prominent portion of Zone HL-1 (8-17%) and *Artemisia* was 0-1.3%. Among aquatic taxa, only *Pediastrum* comprised more than 1%.

Charcoal accumulation rates, with charcoal particles composed primarily of wood rather than grass throughout the record, were high and variable from 8000 to 4000 cal yr BP and less variable from 4000 cal yr BP to the present (Figure 5). Background charcoal levels were initially low at 1.80 particles cm^{-2} yr^{-1} at 7920 cal yr BP. By 6000 cal yr BP, background charcoal levels were consistently above 2.00 particles cm^{-2} yr^{-1} and reached a peak of 3.40 cm^{-2} yr^{-1} at 6930 cal yr BP. Fire-episode frequency, as measured by the distribution of charcoal peaks, was variable over the course of the record but generally higher at the beginning of the record and lower at the end. The highest frequency was 18.22 episodes 1000 yr^{-1}, which occurred at ~8000 cal yr BP. Fire frequencies gradually fell to 9.18 episodes 1000 yr^{-1} at 6330 cal yr BP. Although the signal-to-noise index was high for the entire dataset at 0.79, it was especially high during Zone HL-1, lending confidence to these results.

Zone HL-2 (9.54-4.26 m depth; ca 6300-2000 cal yr BP) pollen was dominated by *Pinus* (38-65%) but these percentages gradually declined over time. Three to 11% of the *Pinus* record was composed of Haploxylon-type *Pinus* and 0.5-3.5% was Diploxylon-type *Pinus*. *Abies* (4-16%) and *Pseudotsuga* (7-18%) percentages rose from the bottom to the top of this zone. Cupressaceae (6-21%) values dropped from higher percentages in Zone HL-1. *Alnus rubra*-type values remained at low levels (0-2.6%), deciduous-type *Quercus* fluctuated from 5-17%, *Salix* ranged from 0-2.6%, and *Artemisia* ranged from 0-2% throughout Zone HL-2. *Pediastrum araneosum* values increased (0-7%) and *P. boryanum* had a significant spike in its occurrence (0.3-92%).

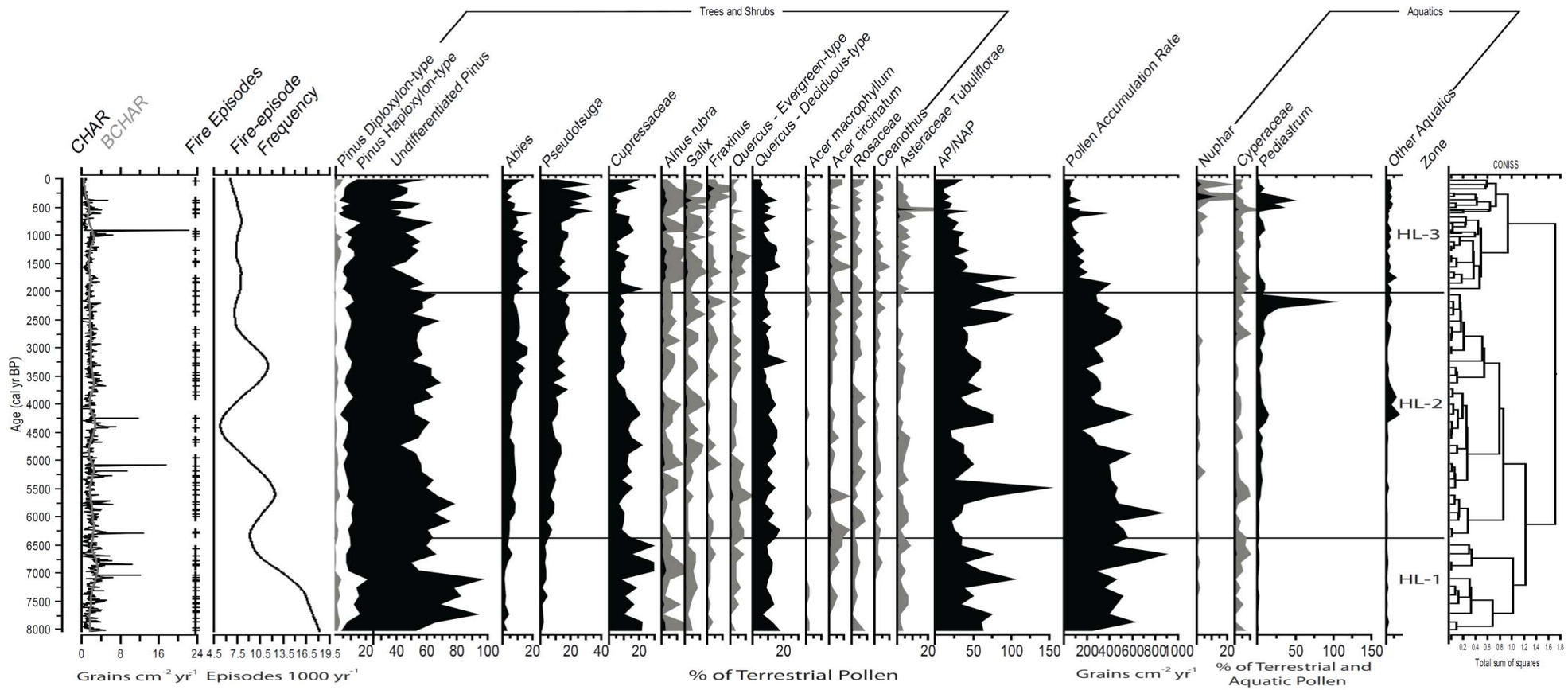

Figure 5. Charcoal and pollen data for selected taxa from Hobart Lake.

PARs spanned from 2265-8223 grains cm^{-2} yr^{-1}. The pollen zone suggests a period of mixed-conifer forest based on its close comparison with modern pollen from the Pacific Northwest (*Minckley and Whitlock*, 2000). Background charcoal levels fluctuated between 1.40 and 2.50 particles cm^{-2} yr^{-1} from 6000 until 800 cal yr BP. Fire frequencies fluctuated around 7-10 episodes 1000 yr^{-1} until around 2500 cal yr BP when they consistently held at 7-8 episodes 1000 yr^{-1}. The charcoal particles were wood rather than grass.

Zone HL-3 (4.26-0.00 m depth; ca 2000-0 cal yr BP) pollen was dominated by *Pinus* (25-54%), although less so than in the other zones. Haploxylon-type represented 4-15% and Diploxylon-type 0-5% of the *Pinus* record. *Abies* (2-16%) levels fluctuated throughout the zone, whereas *Pseudotsuga* (10-32%) levels continued to increase from the previous zone. Cupressaceae (3-21%) levels also fluctuated but remained below the higher levels of Zone HL-1. *Salix* percentages ranged from 0.3%-6.3%. *Fraxinus* and *Salix* occurred in low values throughout the record with the only percentages of note occurring within Zone HL-3 (0-5.7%). Deciduous-type *Quercus* percentages were between 4-17% with no temporal trend, and *Artemisia* levels varied between 0 and 3%. Asteraceae *Tubuliflorae* maintained low percentages (0-1%) throughout Zones HL-1 and HL-2 but saw higher percentages (3.6%) in Zone HL-3. *Pediastrum araneosum* (0-11%) and especially *P. boryanum* (0-47%) reached significant percentages during this time period. PARs ranged from 806 to 8680 grains cm^{-2} yr^{-1} in Zone HL-3. Based on comparison with modern pollen data, the zone marks the establishment of modern mixed-conifer forest at the site (*Minckley and Whitlock*, 2000). Background charcoal levels,

with charcoal composed primarily of wood, dropped from around 2 particles cm^{-2} yr^{-1} to 1.31 particles cm^{-2} yr^{-1} to 0.30 cm^{-2} yr^{-1} by the present day (Figure 5). Fire frequencies dropped slightly from 7-8 episodes 1000 yr^{-1} to the present level of 6.43 episodes 1000 yr^{-1}.

Discussion

The paleoecological data from Hobart Lake and other records from sites in the Pacific Northwest (Table 2, Figure 1) are used to reconstruct the vegetation, fire and climate history of west side of the southern Cascade Range. Within this context, I examined of the history of *Abies* and *Pseudotsuga* to better understand the response of these conifers, which are dominant at Hobart Lake, to past changes in the fire regime and climate. These interpretations were aided by independent paleoclimate records and paleoclimate model simulations for the region (*Barron et al.*, 2003; *Bartlein et al.*, 1998; *Lyle et al.*, 2012; *Mock and Brunelle-Daines*, 1999).

Table 2. Oregon and northern California paleoecological site publications, locations, and elevations referenced in this study.

Publications	**Site**	**Latitude**	**Longitude**	**Elevation (m)**
Worona and Whitlock, 1995	Little Lake	44°10’N	123°35’W	217
Sea and Whitlock, 1995	Indian Prairie Fen	44°38’N	122°34’30”W	988
	Gold Lake Bog	43°39’N	122°02’30”W	1465
Briles et al., 2008	Sanger Lake	41°54'06"N	123°38'49"W	1550
	Bolan Lake	41°.023N	123°.458W	1638
Daniels et al., 2005	Mumbo Lake	41°11'27"N	122°30'36"W	1859
Briles et al., 2011	Cedar Lake	41°12'N	122°27'W	1950
Mohr et al., 2000	Crater Lake	41°24'N	123°35'9W	2288

Vegetation, Fire, and Climate

History of the Southern Cascade Range

Paleoclimate model simulations suggest that conditions during the full-glacial period were colder and drier than at present (*Bartlein et al.*, 1998). At 18,000 cal yr BP a glacial anticyclone around the Laurentide ice sheet created easterly winds over much of North America (*COHMAP*, 1988). The jet stream was pushed southward resulting in cold dry conditions to the north of its location and cold moist conditions to the south. Fire history reconstructions from Little Lake in the Coast Range indicate low fire frequencies, which are consistent with cold dry conditions (*Grigg and Whitlock*, 1998). Other paleoclimate studies suggest that much of coastal California and Oregon became wetter after 14,000 cal yr BP, possibly due to the incursion of moisture from the south (*Lyle et al.*, 2012). A northward shift in the location of the westerlies as the Laurentide ice sheet retreated could have caused an increase in precipitation as well, which would also explain the low fire frequencies seen at this time (*Bartlein et al.*, 1998; *COHMAP*, 1988).

Climate during the Younger Dryas Chronozone (12,900 to 11,500 cal yr BP (*Alley*, 2000)) was characterized by dramatic cooling in some but not all Pacific Northwest records (Figure 6). Isotopic data from Oregon Caves National Monument suggest a rapid 3°C drop at 12,900 cal yr BP and a rise of 4-5°C about 11,700 cal yr BP (*Vacco et al.*, 2005). Another temperature reconstruction based on alkenone data from the ODP 1019 ocean core, taken approximately 50 km off the coast of the Oregon and California border, implies the same rapid fall and rise of temperatures (*Barron et al.*, 2003). Westerly winds from 12,000 cal yr BP onward likely had a greater impact on the

continent everywhere except the vicinity of the ice sheet where the glacial anticyclone's impacts were localized (*COHMAP*, 1988).

Early-Holocene climate was characterized by levels of summer and winter insolation that reached their respective highest and lowest levels of the last 20,000 years (Figure 6) (*Bartlein et al.*, 1998). Model simulations for 11,000 cal yr BP show the direct consequences of the amplified seasonal cycle of insolation that resulted in warmer effectively drier summers and cooler winters in the Pacific Northwest (Figure 7). Indirectly, the northeastern Pacific subtropical high-pressure system expanded as a result of higher-than-present summer insolation, which further suppressed summer precipitation throughout the Pacific Northwest and California region.

Mid-Holocene climate conditions featured waning summer insolation levels (Figure 6). By approximately 6000 cal yr BP model simulations indicate that summers were cooler than before although still warmer than present, although the degree of cooling is debated (*Bartlein et al.*, 1998; *Diffenbaugh*, 2003; *Mock and Brunelle-Daines*, 1999) (Figure 7). The models discussed in Bartlein et al. (1998) indicate a 5°C temperature anomaly in the Pacific Northwest while Diffenbaugh (2003) shows only a 1°C anomaly. The discrepancy may exist due to the different resolutions of the models Bartlein et al. (1998) used a relatively coarse (4.4° latitude to 7.5° longitude) model, whereas the model in Diffenbaugh (2003) was more finely resolved (2.8° latitude x 2.8° longitude).

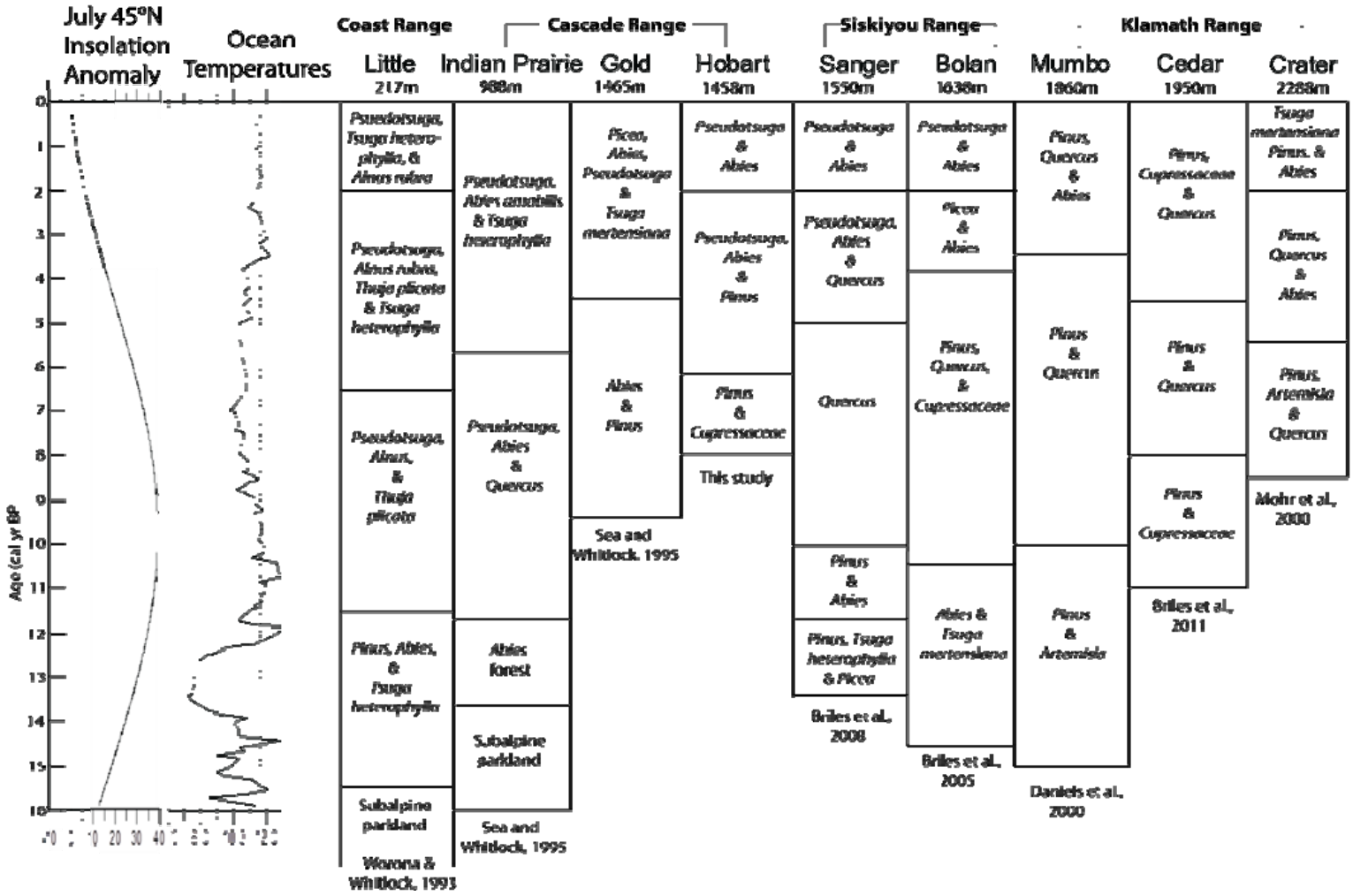

Figure 6. Paleoclimate proxies and vegetation summaries showing July 45°N insolation anomaly (*Berger*, 1978), reconstructed Pacific Ocean sea surfaces temperatures from ODP 1019 off the coast of the California-Oregon border (*Barron et al.*, 2003), and the vegetation history of sites in the Coast Range, Cascade Range, Siskiyou Range and Klamath Range.

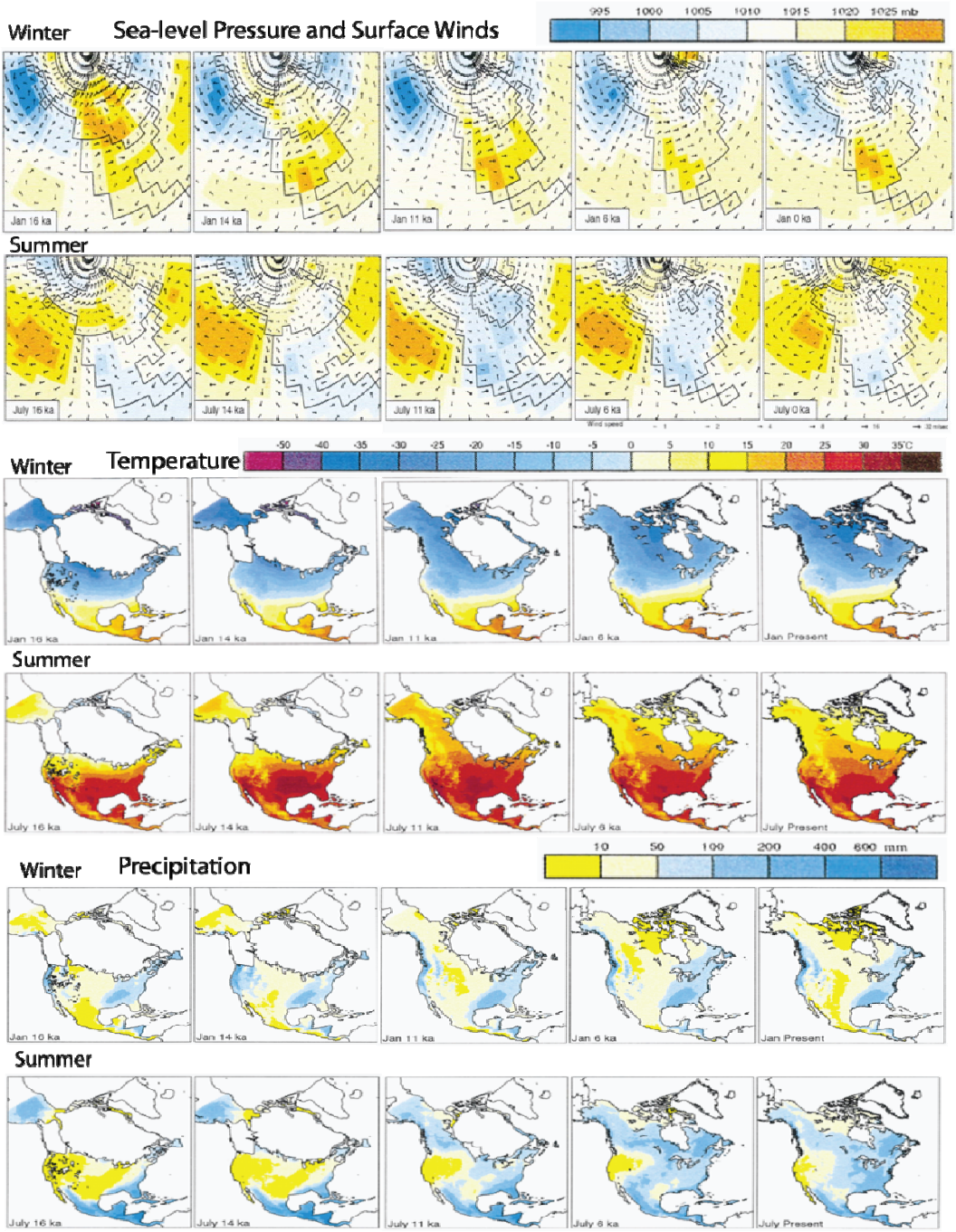

Figure 7. Paleoclimate model simulation results from Bartlein et al. (1998). The top two series of model outputs indicate the changing size and strength of persistent high- and low-pressure systems in the Pacific Ocean by season and year at 16 ka, 14 ka, 11 ka, 6 ka, and the present. Surface wind direction and strength is denoted by the arrow direction and boldness. The middle series of panels show simulated winter and summer temperatures, as controlled by insolation and atmospheric circulation. The lower series display simulated summer and winter precipitation, which is influenced by persistent high and low pressure systems controlled by insolation, the position of the westerlies, and, in the late-glacial period, the influence of the ice sheet.

The 6 ka simulations suggest that the northeastern Pacific subtropical high-pressure system was weakened and summers were less dry than during the early Holocene (*Bartlein et al.*, 1998; *Thompson et al.*, 1993). Winter conditions warmed as well and differences between seasons attenuated compared with the early Holocene, although they were still cooler than the present day (*Diffenbaugh*, 2003). Precipitation was likely similar or slightly lower than present-day values (*Diffenbaugh*, 2003; *Mock and Brunelle-Daines*, 1999).

The climate of the last 3000 years was characterized by cooler and wetter conditions than before. These conditions are attributed to a continuing decrease of summer insolation in the late Holocene and the associated weakening of the northeastern Pacific subtropical high-pressure system (Figure 7) (*Bartlein et al.*, 1998). Within this period, drier conditions occurred in the western United States during the Medieval Climate Anomaly (ca. 900 to 1300 CE; (*Cook et al.*, 2004)), and cooler conditions prevailed during the Little Ice Age (ca. 1400 – 1700 CE; (*Mann et al.*, 2009)).

Vegetation in Oregon and northern California fluctuated in response to changes in climate from the LGM to the present. A full-glacial record from Little Lake in the Coast Range indicates that the landscape supported subalpine parkland with *Pinus*, *Tsuga mertensiana,* and *Picea* (Figure 6) (*Worona and Whitlock*, 1995). A late-glacial record from Indian Prairie Fen in the western Cascade Range also shows that subalpine parkland predominated with *Picea*, *Tsuga heterophylla*, and *Tsuga mertensiana* (*Sea and Whitlock*, 1995). Additional paleoecological records extend to the Younger Dryas Chronozone including Bolan and Sanger lakes (*Briles et al.*, 2008) and Mumbo Lake (*Daniels et al.*,

2005). Despite a drop in temperature observed in speleothem and marine data (*Barron et al.*, 2003; *Vacco et al.*, 2005), pollen records show little evidence of a climate reversal at this time with only slight increases in *Abies*, *Tsuga heterophylla*, and *Tsuga mertensiana* (*Briles et al.*, 2005; *Grigg and Whitlock*, 1998; *Sea and Whitlock*, 1995; *Worona and Whitlock*, 1995). The lack of a vegetation response may be due to the fact that Pacific Northwest conifers are long-lived and may have been fairly insensitive to a relatively brief climate fluctuation. The pollen data from Siskiyou and Klamath ranges features greater amounts of *Pinus* and *Quercus*, which is consistent with paleoclimate model simulations that suggest warmer and dry condition as a result of the summer insolation maximum during the early Holocene (*Briles et al.*, 2005; *Briles et al.*, 2011; *Daniels et al.*, 2005; *Mohr et al.*, 2000; *Sea and Whitlock*, 1995; *Worona and Whitlock*, 1995).

The Hobart Lake pollen record begins at 7900 cal yr BP. The abundance of *Pinus* pollen prior to 6300 cal yr BP, likely from *Pinus ponderosa,* is consistent with early-Holocene drought. The species has high heat and drought tolerances compared with other Pacific Northwest conifers (*Minore*, 1979). *Quercus* comprised a substantial portion of the pollen record from 6300 to 7900 cal yr BP. The species is likely *Quercus garryana*, which must have extended its range to higher elevations based on its high pollen percentages at Hobart Lake compared with the present (*Franklin and Dyrness*, 1988; *Minore*, 1979). Cupressaceae pollen is attributed to either xerophytic *Calocedrus decurrens* or *Juniperus occidentalis*, is present above the lake on an east-facing bluff. Cupressaceae reached its highest percentages at 6300 cal yr BP (Figures 6 and 8). In contrast, mesophytic species, such as *Abies*, that prefer relatively cool and wet conditions

were less abundant from 6300 to 7900 cal yr BP than they were subsequently (*Burns and Honkala*, 1990; *Minore*, 1979).

The charcoal record at Hobart Lake suggests fires were more numerous based on a shorter fire return interval (FRI) and levels of biomass burning were higher based on CHAR levels in the mid-Holocene than at present (Figure 8). The fire return intervals were at their highest at approximately 6280 cal yr BP and increased substantially afterwards. Frequent fires prior to this time may have consumed much of the biomass on the landscape, leaving little fuel to burn in subsequent fires. This is supported by a lower ratio of arboreal to non-arboreal pollen from approximately 6500 to 5700 cal yr BP (Figure 5). However, the generally high FRIs are consistent with paleoclimate model simulations that show winter precipitation at levels similar or slightly less than at present (Figure 8) (*Bartlein et al.*, 1998).

The longer FRI at 6300 cal yr BP favored *Pinus ponderosa* and *Quercus* over *Abies* as evidenced by their pollen abundances (Figure 6). However, Cupressaceae declined abruptly at 6300 cal yr BP (Figure 8). *Calocedrus decurrens* is fairly resistant to fires, especially as trees mature, and *Juniperus occidentalis* is more vulnerable to fire but its bark thickens with age to provides some fire protection (*Agee*, 1993; *Burns and Honkala*, 1990). Additionally, mature stands of *Juniperus occidentalis* can create a vegetation-free zone around themselves by using most of the soil moisture and leaving little for other species, thereby creating a small fire buffer (*Agee*, 1993). *Juniperus occidentalis* and *Calocedrus decurrens* establish themselves well after a fire, although *Calocedrus decurrens* seedlings prefer some shade.

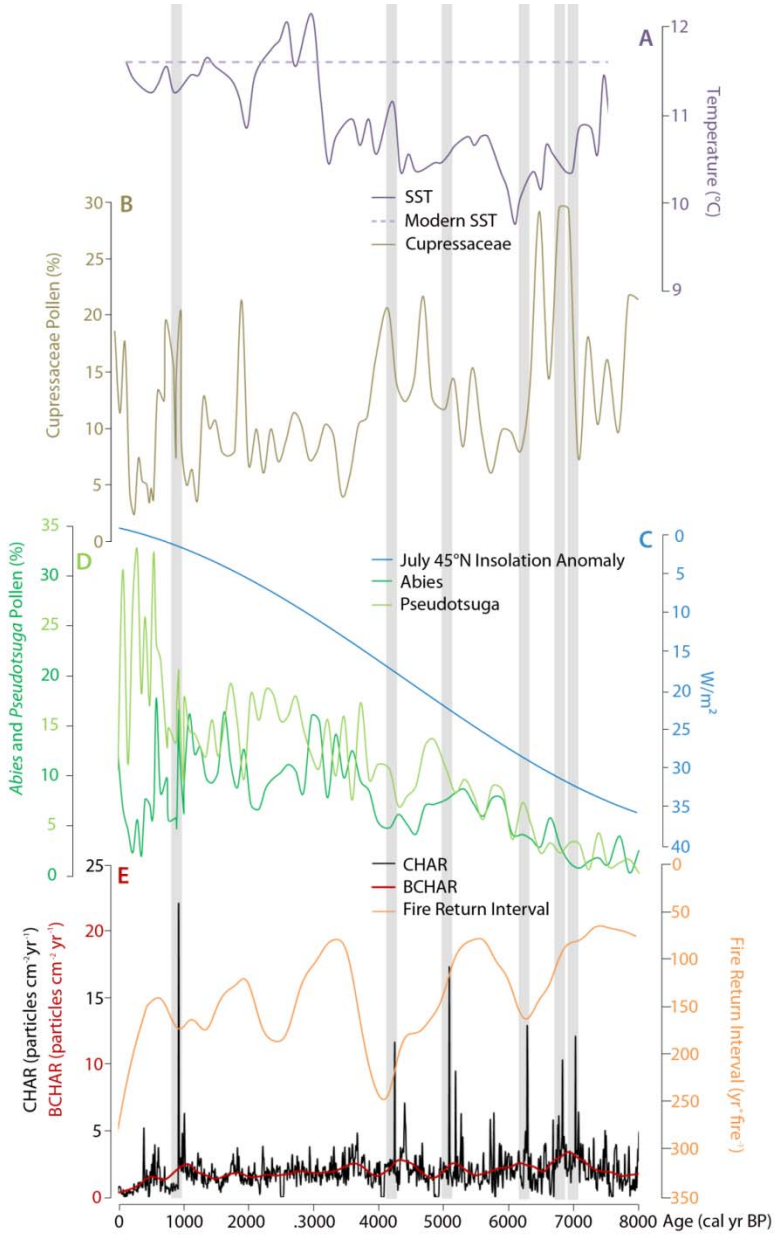

Figure 8. Fire and selected pollen records from Hobart Lake compared with regional environmental proxies. A. Modern and historic sea surface temperatures from ODP 1019 approximately 50 km off the California-Oregon border (*Barron et al.*, 2003). B. Cupressaceae pollen percentages at Hobart Lake. C. The July 45°N insolation anomaly (*Berger*, 1978). D. Pollen percentages of *Abies* (dark green) and *Pseudotsuga* (light green) at Hobart Lake. E. CHAR (charcoal accumulation rate) in black and BCHAR (background charcoal accumulation rate) in red, with the fire return intervals (FRI) in orange at Hobart Lake. The vertical gray bars are aligned with the highest CHAR levels and denote selected fire episodes. They provide a comparison point throughout the fire, climate, and pollen records.

A comparison of FRI and Cupressaceae pollen data at Hobart Lake reveals a complicated relationship between these species, fire and climate (Figure 8). Cupressaceae abundances fluctuated widely and abruptly, suggesting rapid responses of either *Juniperus occidentalis* or *Calocedrus decurrens* to particular fire episodes. However, those responses seem to have varied through time. For example, the fire at approximately 7033 cal yr BP was associated with a decrease in Cupressaceae pollen percentages to 7% beginning at approximately 7024 cal yr BP and then an increase to 29% at about 6878 cal yr BP. The fire event at approximately 6833 cal yr BP occurred when Cupressaceae abundances were at 29%, they remained at this level at least until approximately 6733 cal yr BP, then declined to 14% by about 6580 cal yr BP. After the fire event at approximately 6290 cal yr BP Cupressaceae abundances fell from 13% before the fire episode to 8% afterwards. These abrupt fluctuations in pollen abundances may indicate variations in fire severities wherein some fires caused mortality, others promoted tree establishment and still others resulted in little change in Cupressaceae. Also, *Calocedrus decurrens* is more susceptible to pocket dry rot (*Tyromyces amarus*) after being damaged in a fire at present, which could have delayed mortality as seen after the fire at approximately 6833 cal yr BP (*Burns and Honkala*, 1990).

The fluctuations in Cupressaceae pollen at Hobart Lake may have been a response to changes in climate as well. *Juniperus* today establishes during warm and dry periods, and *Calocedrus decurrens* can live in dry areas that receive only 38 cm per year (*Burns and Honkala*, 1990; *Lyford et al.*, 2003). Paleoclimate model simulations for 6000 cal yr BP indicate conditions were warmer than the present when Cupressaceae generally

represented 10% or more of the Hobart Lake record (*Bartlein et al.*, 1998). At Sanger Lake 100 km west of Hobart, Cupressaceae pollen was attributed to *Calocedrus decurrens*, and these percentages increased at times when fires were more frequent and decreased when it was less frequent (*Briles et al.*, 2008). The less clear relationship between fire and Cupressaceae at Hobart Lake may reflect the unique location of *Juniperus occidentalis* at its western boundary where wet conditions and competition may have limited its expansion. Alternatively, the Cupressaceae record at Hobart Lake may have resulted from changes in abundance of both *Juniperus occidentalis* and *Calocedrus decurrens* and may have been largely controlled by changes in fire activity.

From 6300 to 2000 cal yr BP, *Pinus* and Cupressaceae levels at Hobart Lake decreased and *Abies* and *Pseudotsuga* became abundant (Figure 9). This shift is likely the result of the transition from warm dry conditions in the early Holocene and mid-Holocene to cooler wetter conditions in the late Holocene (*Burns and Honkala*, 1990; *Minore*, 1979). The charcoal record between 6300 and 2000 cal yr BP indicates that FRIs fluctuated from 77.6 to 247.2 years per fire, with an overall decline in fire activity. CHAR, BCHAR, and fire frequency levels at Hobart Lake also declined abruptly at about 4000 cal yr BP suggesting fires became infrequent. In contrast, the Mumbo Lake charcoal record from the Klamath Mountains record the interval between ca. 4200 and 3800 cal yr BP as having one of the highest fire frequencies of the Holocene (*Mohr et al.*, 2000). The generally declining trend of fire occurrence at Hobart Lake is probably related to the long-term changes in climate toward cooler wetter conditions. However, on

sub-millennial scales, fire frequency was more variable, which, in addition to climate, can be attributed to changes in fuel structure and composition.

In the last 2000 years, *Pinus* percentages at Hobart Lake were at their lowest levels of the record, Cupressaceae values were low, and *Abies* and *Pseudotsuga* values were high (Figures 6 and 9). CHAR and BCHAR levels rose from 1100 to 700 cal yr BP, which falls within the Medieval Climate Anomaly (ca. 900 to 1300 CE) (*Cook et al.*, 2004). A large charcoal peak occurred at about 900 cal yr BP, indicating a large fire episode, and interestingly, large charcoal peaks also registered at approximately 900 cal yr BP at Bolan and Sanger lakes (*Briles et al.*, 2011). FRIs averaged about 150 years per fire episode until 600 cal yr BP when the FRIs rapidly increased, likely due to cooler and wetter conditions during the Little Ice Age (ca. 1400 – 1700 CE; (*Mann et al.*, 2009)).

The fire and vegetation data from Hobart Lake are consistent with our understanding of Holocene climate history and particularly the influences that slowly varying changes in the seasonal cycle of insolation have on regional climate (Figures 7 and 8). The expansion of xerophytic taxa and the short FRIs at Hobart Lake from approximately 7900 to 5500 cal yr BP occurred during warm dry conditions caused by higher-than-present summer insolation levels and a strengthened subtropical high-pressure system in the early and mid-Holocene. The increase in mesophytic vegetation and decline in fire frequency in the last 4000 years is evidence of cooler and wetter conditions related to declining summer insolation, although the Medieval Climate Anomaly stands out as a time of anomalously warmer and drier conditions and features

one of the most significant fire events in Hobart Lake's record while the cooler and wetter conditions of Little Ice Age caused increased fire return intervals.

History of *Abies* and *Pseudotsuga* in Oregon and Northern California

A comparison of pollen records from sites west of the Cascade crest in Oregon and northern California help clarify the history of *Abies* and *Pseudotsuga,* two of the dominant conifers in the region. In parts of the Pacific Northwest, *Abies* pollen comes from *A. amabilis* (Pacific silver fir), *A. grandis*, *A. concolor*, or *A. magnifica* (California red fir) (Figure 9). Each species at present has slightly different climate requirements and different strategies for coping with fire. *A. amabilis*, while abundant in coastal British Columbia, resides at higher elevations (1000 to 1500 m elevation) in the southern Cascade Range as it prefers relatively cool wet conditions (*Burns and Honkala*, 1990; *Franklin and Dyrness*, 1988; *U.S. Geological Survey*, 2006). The species is found in areas that average 150 cm of precipitation a year and have winter snow accumulations of over 760 cm (*Burns and Honkala*, 1990). Although *A. amabilis* grows in a summer-dry climate, it needs moist soils year-round as it does not tolerate drought well (*Burns and Honkala*, 1990; *Minore*, 1979). Infrequent, high-severity fire regimes are characteristic of forests in which *A. amabilis* resides (*Agee*, 1993). Its thin bark and shallow roots make the species especially susceptible to fire.

The range of *Abies grandis* extends east of the Cascade Range in northern Oregon and Washington but primarily remains west of the Cascade Range in southwestern Oregon and northern California. *A. grandis* is largely restricted to low-elevation coastal

settings, although small populations grow at mid-elevations around Bolan and Hobart lakes (Figure 9) (*U.S. Geological Survey*, 2006). *A. grandis* grows in areas averaging 51 to 254 cm of precipitation per year, with most falling in winter. It is known to be a moderate fire resister, occupying areas that burn infrequently and only under the most severe conditions, such as riparian areas (*Burns and Honkala*, 1990). In drier settings, such as hillside slopes, *A. grandis* adapts to frequent fires by growing deeper roots and thicker bark.

The range of *Abies concolor* extends farther south than that of the other three *Abies* species and *A. concolor* is abundant in the Sierra Nevada and southern Cascade Range (Figure 9). These areas receive 51 to 89 cm of precipitation per year on average, and the lower moisture levels are consistent with *A. concolor*'s more inland distribution (*Burns and Honkala*, 1990). Seedlings are highly susceptible to fire, but become more resistant with age (*Agee*, 1993; *Burns and Honkala*, 1990).

Abies magnifica is a high-elevation species that prefers moist and cool to cold climates where temperatures rarely exceed -30°C in the winter or 30°C in the summer (*Burns and Honkala*, 1990). It lives in areas receiving 75 to 150 cm of moisture per year, 80% of which falls as snow. Forests dominated by *A. magnifica* have a moderate-severity fire regime; young trees are susceptible to fires but acquire some resistance with age as their bark thickens (*Agee*, 1993).

Pseudotsuga menziesii var. *menziesii* has a distribution that extends from British Columbia to northern California (Figure 10). This subspecies lives under a range of climatic conditions with precipitation levels ranging from < 30 cm to > 700 cm per year

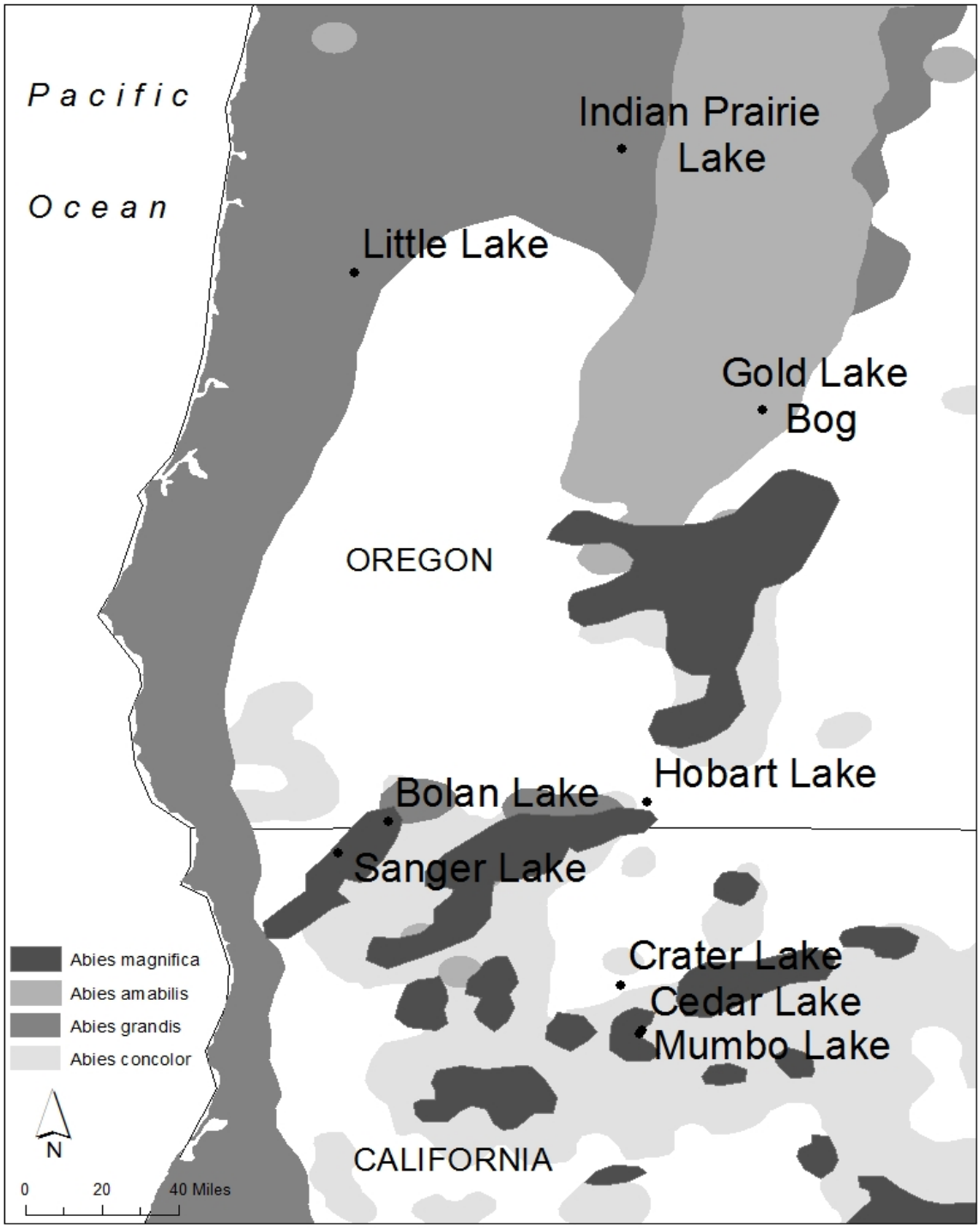

Figure 9. Distribution of four *Abies* species in western Oregon and northern California (*U.S. Geological Survey*, 2006).

(*Thompson et al.*, 1999). As with *Abies concolor*, young *Pseudotsuga* are vulnerable to fires but older trees (>100-150 years) develop thick bark that resists ground fires (*Burns and Honkala*, 1990).

Nine pollen records were used to reconstruct the history of *Abies* and *Pseudotsuga*. Little Lake is the lowest elevation site and is located in the Oregon Coast Range 45 km east of the Pacific Ocean and 40km west of the Willamette Valley (Figures 1 and 6) (*Worona and Whitlock*, 1995). Presently, it is surrounded by a mixed forest of *Pseudotsuga menziesii*, *Thuja plicata* (western red cedar), and *Tsuga heterophylla* (*Franklin and Dyrness*, 1988). The Little Lake pollen record extends back more than 40,000 years, but only the last 16,000 years was considered for this comparison. Indian Prairie Fen is located in the western Cascade Range, 100 km northwest of Little Lake (*Sea and Whitlock*, 1995). The site is characterized by *Pseudotsuga menziesii*, *Abies procera* (noble fir), *Abies amabilis*, *Tsuga heterophylla*, and *Taxus brevifolia* (Pacific yew), and the record covers the last 14,000 years. Gold Lake Bog on the eastern slope of the Cascade Range lies 120 km south southwest of Indian Prairie Fen. Its record begins at 9950 cal yr BP and the modern site is dominated by *Pseudotsuga menziesii*, *Tsuga mertensiana* (mountain hemlock), *Pinus monticola*, *Pinus contorta*, and *Abies amabilis*. Sanger Lake lies in the Siskiyou Mountains, a subrange of the Klamath Mountains, 100 km west southwest of Hobart Lake (*Briles et al.*, 2008). It is surrounded by *Abies concolor*, *Picea breweriana* (Brewer spruce), *Chamaecyparis lawsoniana* (Port-Orford cedar), *Pinus monticola*, and *Pseudotsuga menziesii* (*Briles et al.*, 2008; *Franklin and Dyrness*, 1988). The Sanger Lake record extends to 14,000 cal yr BP. Nearby Bolan

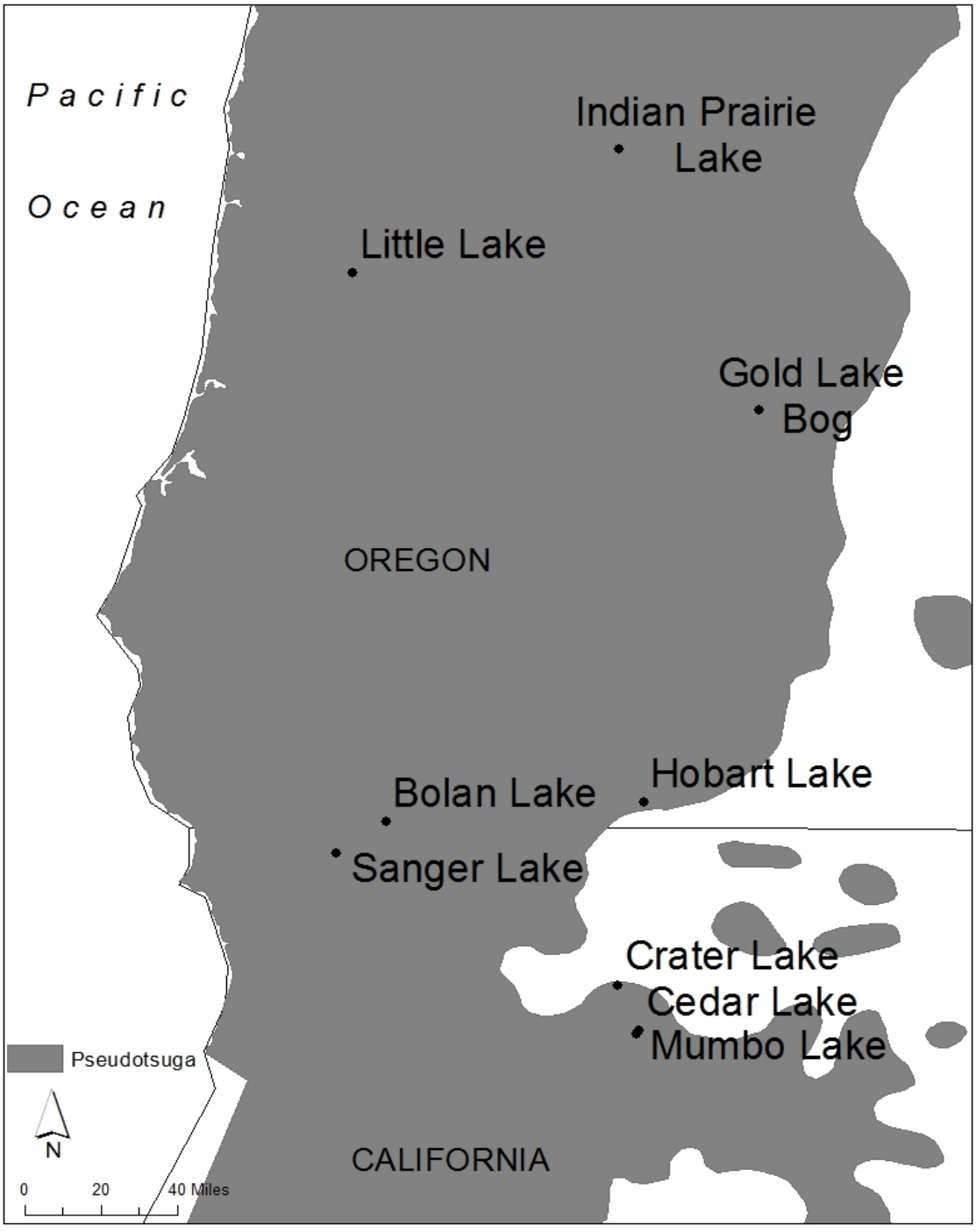

Figure 10. Present-day *Pseudotsuga menziesii* distribution in western Oregon and northern California (*U.S. Geological Survey*, 2006).

Lake in the Siskiyou Mountains is just 20 km northwest of Sanger Lake (*Briles et al.*, 2008). Its more inland location creates a slightly warmer drier climate and supports a forest of *Abies concolor*, *Pinus monticola*, and *Pseudotsuga menziesii*. This record covers the last 16,000 years. Mumbo Lake in the Klamath Mountains lies 120 km southwest of Bolan Lake (*Daniels et al.*, 2005). It is surrounded by a mixed-conifer forest of *Pinus contorta* var. *murrayana* (Sierran lodgepole pine), *Abies concolor*, *Abies magnifica*, *Pinus monticola*, and *Tsuga mertensiana*, and the pollen record spans the last 15,217 years. Cedar Lake is just 2 km northwest of Mumbo Lake, and the watershed is underlain by ultramafic soils whereas Mumbo Lake is not (*Briles et al.*, 2011). Therefore, the forest composition at Cedar Lake is dominated by *Pinus jeffreyi* and *Calocedrus decurrens*. This record spans approximately the last 11,000 cal yr BP. Also surrounded by ultramafic soils, Crater Lake is 20 km north northwest of Cedar Lake (*Briles et al.*, 2011; *Mohr et al.*, 2000). The dominant conifers include *Pinus balfouriana* (foxtail pine), *Pinus albicaulis* (whitebark pine), *Pinus monticola*, *Pinus contorta*, *Abies magnifica*, and *Tsuga mertensiana* and the record covers 8000 cal yr BP (*Mohr et al.*, 2000).

At approximately 15,000 cal yr BP, warming conditions led to a shift from subalpine parkland to closed montane forest dominated by *Abies* (*Grigg and Whitlock, 1998; Worona and Whitlock, 1995*). Between 14,500 and 13,000 cal yr BP, warmer wetter conditions allowed *Abies* to shift its range upslope by 300 to 500 m and become established at Sanger, Bolan, and Mumbo lakes (Figure 11) (*Briles et al.*, 2005; *Daniels et al.*, 2005). Forests were more closed at this time as well, as suggested by the increase

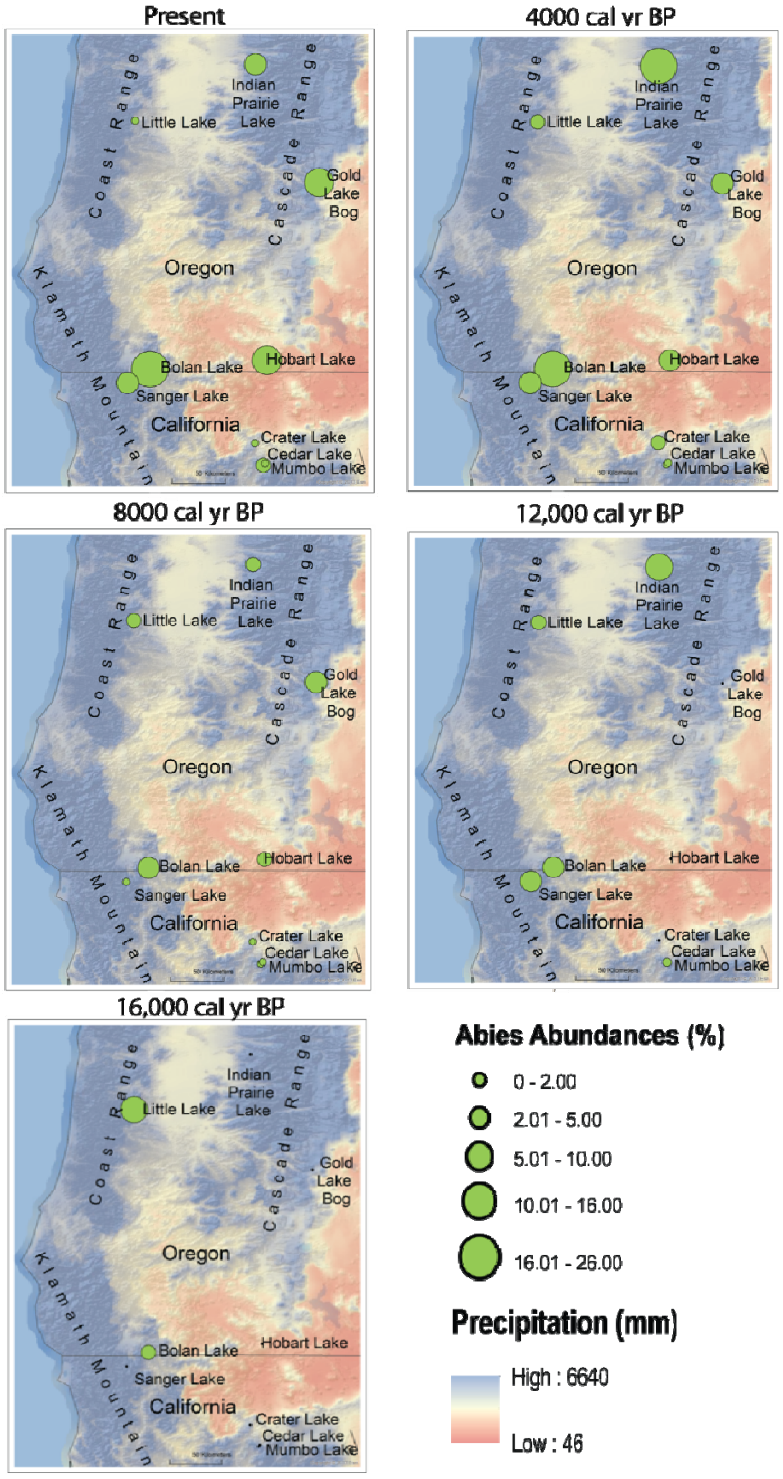

Figure 11. *Abies* pollen percentages at paleoecological sites in western Oregon and northern California. The green dot indicates *Abies* pollen abundance (%). A black dot at a site indicates that the pollen record does not extend that far back in time and *Abies* abundance is therefore unknown. The background map displays average annual precipitation from 1981 – 2010 (*PRISM Climate Group*, 2014).

of *Tsuga* and *Abies* percentages in the lake-sediment records at Bolan Lake (*Briles et al.*, 2008).

At Little Lake, *Abies* declined in importance through the Younger Dryas Chronozone and *Pinus* and *Pseudotsuga* increased (Figure 11) (*Worona and Whitlock*, 1995). At Indian Prairie Fen, *Abies* abundance increased by 12,000 cal yr BP to become a substantial portion of the landscape, which suggests a general warming trend towards the end of the Younger Dryas Chronozone (*Sea and Whitlock*, 1995). Although not as dramatic, Bolan Lake showed a similar increase by 12,000 cal yr (*Briles et al.*, 2008; *Briles et al.*, 2011). Thus, the cooler temperatures of the Younger Dryas Chronozone, though short-lived, may have been detrimental to *Abies* at low elevations and favored its expansion at mid-elevations across western Oregon and northern California.

At 8000 cal yr BP, *Abies* pollen dropped to <10% of the pollen record at Little Lake and remained at low levels through the early and mid-Holocene (Figure 11) (*Worona and Whitlock*, 1995). Indian Prairie Fen supported an *Abies*-dominant forest until 10,000 cal yr BP; after that, its percentages declined dramatically to the lowest of the record by 8000 cal yr BP (*Sea and Whitlock*, 1995). *Abies* pollen levels gradually rose after this point as the climate cooled. The Gold Lake Bog record had low values of *Abies* at the start of its record at 9500 cal yr BP and this pattern continued through the early and mid-Holocene (*Sea and Whitlock*, 1995). *Abies* pollen abundances at Hobart Lake were low initially but steadily increased during the mid-Holocene. Both Sanger and Bolan lakes in the Siskiyou Range recorded declining abundances of *Abies* pollen between 12,000 and 8000 cal yr BP as *Pinus* and *Cupressaceae* increased (*Briles et al.*, 2008). *Abies* percentages at

Mumbo Lake and Cedar Lake declined to negligible levels by 8000 cal yr BP when *Quercus* expanded, and they became more abundant by 5000 cal yr BP (*Briles et al.*, 2011; *Daniels et al.*, 2005). Cedar Lake had extremely low *Abies* pollen levels in the early Holocene but abundance increased slightly in the mid-Holocene (*Briles et al.*, 2011). The low *Abies* levels at this site were likely due to the infertile ultramafic substrate (*Briles et al.*, 2011). Only 20 km from Cedar Lake and 300 m higher, *Abies* pollen was more abundant at Crater Lake during the mid-Holocene, especially after 4000 cal yr BP (*Mohr et al.*, 2000).

At 4000 cal yr BP, *Abies* pollen percentages at Little Lake remained low but reached over 10% of the record by 1500 cal yr BP (Figure 11) (*Worona and Whitlock*, 1995). *Abies* pollen percentages at Indian Prairie Fen fluctuated throughout the late Holocene and showed a short-lived increase in abundance around 4000 cal yr BP (*Sea and Whitlock*, 1995). *Pseudotsuga* and *Abies*, along with *Tsuga heterophylla*, were the dominant species at this site during the last 4000 years. Gold Lake Bog, Hobart Lake, and Sanger Lake experienced a similar rise in the dominance of *Abies* during the late Holocene (*Briles et al.*, 2008; *Sea and Whitlock*, 1995). At Bolan Lake, *Abies* also became more widespread in the late Holocene, and Mumbo Lake in the Klamaths saw a slow rise in *Abies* abundances over the latter half of the Holocene (*Daniels et al.*, 2005). Although always low in abundance, *Abies* pollen percentages increased over the last 2000 years at Cedar Lake (*Briles et al.*, 2011). At Crater Lake, *Abies* remained a low component of the vegetation in the late Holocene (*Mohr et al.*, 2000).

In summary, changes in *Abies* pollen abundances provide information about shifts in its distribution through time. *Abies* represented as much as 30% of the pollen record at Little Lake from 16,000 to 40,000 cal yr BP, and then suddenly declined to less than 10% of the record by 12,000 cal yr BP (Figure 11) (*Worona and Whitlock*, 1995). Therefore, members of the genus thrived in the central Coast Range during the pre-glacial and glacial interval. The shift in climate to warmer and wetter conditions after about 16,000 cal yr BP resulted in a contraction of the *Abies* distribution in the Coast Range, and *Abies* (likely *A. grandis*) was not abundant in this area until 2000 cal yr BP. A significant expansion of *Abies* (inferred to be *A. amabilis*) occurred at Indian Prairie Fen in the Cascade Range during the late-glacial, and its abundance declined and was likely restricted to higher elevations. At mid-elevation Cascade Range sites, Indian Prairie Fen and Gold Lake Bog, *Abies* became more abundant after 8000 cal yr BP (Figure 11) (*Sea and Whitlock*, 1995; *Worona and Whitlock*, 1995). This trend is also noted at Hobart Lake in the southern Cascade Range. In the Siskiyou Range, Bolan and Sanger lakes suggest a remarkably similar *Abies* history, although the species may have been *A. concolor*, *A. grandis*, *A. magnifica*, or some combination of the three (*Briles et al.*, 2008). The pollen data suggest that *Abies* was present through the Holocene, although its abundance changed as its distribution shifted upslope in the early Holocene and downslope in the mid- and late Holocene. More frequent fires in the early Holocene may also have contributed to its decline at low and middle elevations, and it expanded its range in the late Holocene as fire activity decreased. In contrast, *Abies* was never abundant in sites in the Klamath Mountains probably because site elevations are above

the range of most *Abies* species and the conifer is not well adapted to the ultramafic soils (*Briles et al.*, 2011; *Daniels et al.*, 2005; *Franklin and Dyrness*, 1988; *Mohr et al.*, 2000). Regardless, patterns of abundance were similar to those found elsewhere, inasmuch as *Abies* was abundant during the late glacial, its range and/or abundance contracted during the early Holocene, and it gradually became more widespread and abundant during the mid- and late Holocene. These fluctuations throughout the late-glacial and Holocene show the strong preference of *Abies* for cooler climates and lower fire frequency, especially at mid-elevations.

Pollen records of *Pseudotsuga* reveal a different biogeographic history. During the late-glacial period, *Pseudotsuga* was absent at Little Lake before 16,000 cal yr BP, then suddenly represented 10% of the pollen record thereafter (Figure 12) (*Worona and Whitlock*, 1995). During the Younger Dryas Chronozone, it increased in abundance, representing between 20 and 30% of the pollen record. At Indian Prairie Fen in the Cascade Range, *Pseudotsuga* pollen was present by 12,000 cal yr BP, although in low percentages (*Sea and Whitlock*, 1995). *Pseudotsuga* pollen is registered at Bolan and Sanger lakes when the records began at 16,000 and 14,000 cal yr BP, respectively, but in greater abundance at Bolan Lake (*Briles et al.*, 2005). At Mumbo Lake, *Pseudotsuga* was not present in the pollen record at any period, and at Cedar Lake, *Pseudotsuga* was a minor component of the vegetation based on pollen percentages that never exceed 1.5% (*Briles et al.*, 2011).

By 8000 cal yr BP, *Pseudotsuga* pollen became more abundant than before at Little Lake (Figure 12) (*Worona and Whitlock*, 1995). At Indian Prairie Fen,

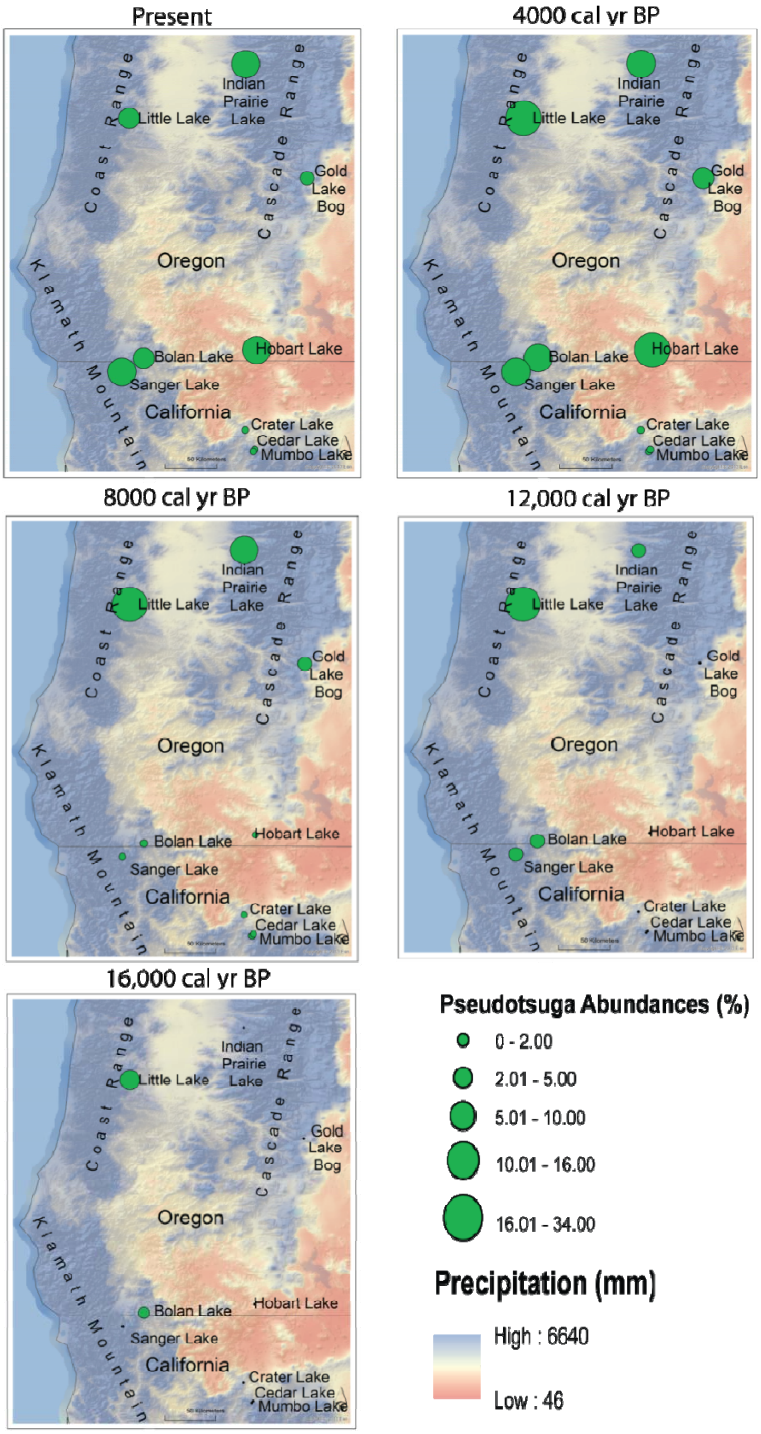

Figure 12. *Pseudotsuga* pollen percentages at paleoecological sites in western Oregon and northern California. Green dots indicate *Pseudotsuga* pollen abundance (%). A black dot at a site indicates that the pollen record does not extend that far back in time and *Pseudotsuga* abundance is therefore unknown. The background map displays average annual precipitation from 1981 – 2010 (*PRISM Climate Group*, 2014).

Pseudotsuga levels fluctuated widely but obtained their highest levels by 8000 cal yr BP (*Sea and Whitlock*, 1995). The Gold Lake Bog record began at 9500 cal yr BP and *Pseudotsuga* was never abundant at this mid-elevation site. Both Sanger and Bolan lakes record declining abundances of *Pseudotsuga* pollen after 8000 cal yr BP (*Briles et al.*, 2008). At Cedar Lake, trace amounts of *Pseudotsuga* pollen were present between 11,000 and 9500 cal yr BP but not afterwards (*Briles et al.*, 2011). Thus, north-south contrasts in the history of Pseudotsuga are first evident at 12,000 cal yr BP, with high values at Little Lake and low values at Bolan and Sanger lakes. The contrast became more apparent after 8000 cal yr BP with *Pseudotsuga* being noticeably more abundant in the Coast and western Cascade ranges than in the Klamath and Siskiyou ranges (Figure 12). The sites where *Pseudotsuga* was abundant in the early Holocene are generally wet sites.

Pseudotsuga pollen levels at Little Lake remained highly abundant at 4000 cal yr BP (Figure 12) (*Worona and Whitlock*, 1995). At Indian Prairie Fen, *Pseudotsuga* pollen remained abundant throughout the mid-Holocene (*Sea and Whitlock*, 1995). At Gold Lake Bog, *Pseudotsuga* pollen levels were low at around 5% at 4000 cal yr BP. *Pseudotsuga* pollen abundances at Hobart, Sanger, and Bolan lakes became steadily more abundant during the middle Holocene. At the ultramafic site Cedar Lake, *Pseudotsuga* was essentially absent from 9500 to 5500 cal yr BP, although it reappeared after this time (*Briles et al.*, 2011). *Pseudotsuga* pollen was hardly present at Crater Lake, only once reaching even 1% of the record (*Mohr et al.*, 2000). The north-south pattern was no longer evident in the data by 4000 cal yr BP as *Pseudotsuga* was abundant region-wide

with the exception of the high elevation sites in the Klamath Mountains. The wetter conditions associated with a reduction in summer insolation levels and a likely southward shift in the Pacific Northwest trough may be one explanation for this pattern, especially at the drier southern sites (*Bartlein et al.*, 1998; *Diffenbaugh*, 2003). Fewer fires associated with greater summer precipitation may have contributed to increased survival of young *Pseudotsuga* as well. This trend is seen between 3400 and 1600 cal yr BP when CHAR and BCHAR levels were low (Figure 8).

In the late Holocene, *Pseudotsuga* levels spiked to 41% at 1200 cal yr BP at Little Lake following a Holocene low of 6% at 2000 cal yr BP, and decreased towards the present (Figure 12) (*Worona and Whitlock*, 1995). *Pseudotsuga* pollen percentages at Indian Prairie Fen increased after 2500 cal yr BP and although *Pseudotsuga* was less important at Gold Lake Bog than at Indian Prairie Fen, Gold Lake Bog also registered a late-Holocene rise in *Pseudotsuga* abundance (*Sea and Whitlock*, 1995). At Hobart Lake, *Pseudotsuga* pollen flourished in the late Holocene, reaching its highest levels of the record (32%) at 560 cal yr BP (Figure 8). *Pseudotsuga* increased in abundance at Bolan and Sanger lakes as well, although not as dramatically as at Hobart Lake (*Briles et al.*, 2008). While substantially less abundant, Cedar Lake had a similar increase in *Pseudotsuga* over the last 2000 years and reached noticeable levels by 1700 cal yr BP (*Briles et al.*, 2011). Crater Lake shows a minor presence of *Pseudotsuga* pollen over the last 3000 years but the conifer probably did not grow on the ultramafic substrates (*Mohr et al.*, 2000).

Close examination of *Abies* and *Pseudotsuga* pollen percentages associated with the 900 cal yr BP fire event at Hobart Lake suggests that both species abruptly declined after the fire event and recovered over the next several hundred years (Figure 8). Subsequent fires at Hobart Lake at about 700 cal yr BP may have caused a further decline in *Abies*, whereas *Pseudotsuga* increased in abundance. A combination of warm dry conditions and fire during the MCA may explain why *Pseudotsuga* expanded at the expense of *Abies* between 700 and 400 cal yr BP. The fact that *Abies* and *Pseudotsuga* abundances were so similar over the course of the Hobart Lake record but deviated markedly after 600 cal yr BP suggests that differing responses to fire caused the decline in *Abies*, especially given the genera's divergent responses to past fire events.

As with *Abies,* examining the pollen record of *Pseudotsuga* assists in understanding the species distributional changes in response to climate through time. Little Lake shows that *Pseudotsuga* was uncommon until the early Holocene (*Worona and Whitlock*, 1995). Worona and Whitlock [1995] speculated that a glacial refugium for *Pseudotsuga* existed to the south of Little Lake and that the species migrated northward during the late-glacial period, becoming widely distributed in the Coast Range by 12,000 cal yr BP. This analysis supports that hypothesis, inasmuch as *Pseudotsuga* pollen is present at the beginning of the Bolan and Sanger lake records which extend into the late-glacial. As these were themselves glaciated, any refugia would have likely been at lower elevations during the LGM. Regardless, warm dry conditions in the early Holocene seem to have allowed *Pseudotsuga* to become the dominant species in the central Coast Range by 7300 cal yr BP. A similar, although less dramatic, pattern was seen in the western

Cascade Range at Indian Prairie Fen (*Sea and Whitlock*, 1995). As temperatures cooled and fires became less frequent in the mid-Holocene, *Pseudotsuga* became less abundant in the Coast and Cascade ranges (*Sea and Whitlock*, 1995; *Worona and Whitlock*, 1995). Additional moisture at these wet sites may not have favored this drought-tolerant species (*Minore*, 1979). *Pseudotsuga* was not abundant on the drier eastern side of the Cascade Range based on its low representation at Gold Lake Bog (*Sea and Whitlock*, 1995). In the southern Cascade Range, *Pseudotsuga* was barely present (1-2% of the pollen) when the Hobart Lake record began at ca. 8000 cal yr BP, suggesting that climate at mid-elevations was not ideal for the species during the early Holocene. By 900 cal yr BP, however, it was one of the dominant species at the site. Nearby Siskiyou Range sites, Bolan and Sanger lakes, show a similar distribution pattern to that of Hobart Lake with the additional benefit of lengthier records (*Briles et al.*, 2008). At those sites, *Pseudotsuga* was present in consistently low levels throughout the late-glacial and early-Holocene periods, implying that the species was able to maintain small populations on the landscape in line with its broad climate tolerances. It was not until the late-Holocene period that climate and fire conditions were ideal for *Pseudotsuga*. In contrast, *Pseudotsuga* is absent from the Mumbo Lake record farther south in the Klamath Mountains and barely registered in the pollen records at Cedar and Crater lakes (*Briles et al.*, 2011; *Mohr et al.*, 2000). Like *Abies*, *Pseudotsuga* is not well adapted to the challenges of growing on ultramafic soils. Despite the species' broad climate tolerances, it seems to prefer a specific set of climatic conditions. These conditions have occurred when northern low-elevation sites, that typically receive high amounts of precipitation,

received less precipitation than present and when southern mid-elevation sites, that usually receive comparatively less precipitation than the northern sites, received precipitation amounts approximating those of the present.

Conclusions

Hobart Lake provides a high-resolution Holocene history of vegetation and fire from the west side of the southern Cascade Range. The record, which spans the last 8000 years, shows changes consistent with large-scale variations in the climate system, suggesting that slowly varying changes in the seasonal cycle of insolation and the indirect effects of insolation on the size and strength of the northeastern Pacific subtropical high-pressure system were important drivers of millennial-scale vegetation change in this region. During the early and mid-Holocene, when the climate was warm and dry, xerothermic species, such as *Pinus ponderosa, Juniperus occidentalis,* and *Calocedrus decurrens*, were more abundant than at present and fires were more frequent that today. With cooler and wetter conditions during the late Holocene, mesophytic taxa, such as *Abies*, flourished and fire frequency declined. At finer temporal scales, different taxa displayed more nuanced responses as demonstrated by fluctuations in Cupressaceae, *Abies* and *Pseudotsuga* pollen in response to changing fire activity. During a very large fire episode at 900 cal yr BP both *Abies* and *Pseudotsuga* decreased in abundance. However, in response to prior fire episodes the species showed divergent responses with *Abies* decreasing after fires and *Pseudotsuga* increasing (Figure 8). Thus on submillennial time scales, changes in fuel biomass, providing more or less fuel for fires,

and short-term climate changes, such as the Medieval Climate Anomaly or Little Ice Age, may explain these fluctuations.

The Holocene history of *Abies* and *Pseudotsuga* shows patterns of changing abundance and distribution in southwestern Oregon and northern California. These patterns reflect changes in fire regimes and climate as well as site-specific differences related to elevation. *Abies* is not well adapted to fire and a clear affinity for cool climates through time, as evidenced by its early Holocene decline and its mid- and late-Holocene expansion. The broad climate range of *Pseudotsuga* has allowed it to survive in western Oregon and northern California through the glacial period, the warm and dry early Holocene, and the cooler and wetter late Holocene. Abundance changes in *Pseudotsuga* through time indicate that the species proliferated at northern low-elevation sites in the Coast Range and central Cascade Range during the early Holocene and then became more abundant at southern drier mid-elevation sites in the southern Cascade and Siskiyou ranges in the late Holocene. The drying of moist sites provided *Pseudotsuga* with opportunities for colonization when the climate was warmer and drier than at present in the early Holocene. In contrast, it was not until the late Holocene that dry sites had sufficient moisture to support *Pseudotsuga*.

The paleoecologic record suggests that the forests of the southern Cascade Range were highly sensitive to changes in climate and fire frequency, and similar changes can be anticipated moving forward. Temperatures are expected to rise in this region 1.7°C to 5.8°C by 2100, with more of this warming occurring during the summer than winter (*Cayan et al.*, 2006; *Mote and Salathé Jr*, 2010). Although some areas of North America

such as the eastern United States are expected to have greater precipitation by mid-century, climate models are less clear on precipitation levels in the southern Pacific Northwest (*Cayan et al.*, 2006; *IPCC*, 2007). Some models suggest a slight increase (1-2%), some a substantial increase (15-20%), while others predict decreases (*Leung et al.*, 2004; *Mote and Salathé Jr*, 2010). Most agree that the region's winter-wet summer-dry precipitation regime will remain intact for the foreseeable future with the majority of yearly moisture from north Pacific storms (*Cayan et al.*, 2006). In fact, some models predict winters will become wetter and summers drier (*Leung et al.*, 2004; *Mote and Salathé Jr*, 2010). Models agree that as temperatures rise throughout this century, more winter moisture will likely fall as rain rather than snow (*Cayan et al.*, 2006; *Leung et al.*, 2004). Consequently, snowpack depths at higher elevations are expected to decline earlier in the spring, likely resulting in a reduction in conifer growth and regeneration and contributing to an increase in fire frequency, along with drier summers. Fire risk is forecast to increase substantially region-wide, with some models projecting potential increases in burn area of as much as 100% by 2085 (*Cayan et al.*, 2006; *Westerling et al.*, 2011). Vegetation models suggest that mid-elevation conifer forest, as seen at Hobart Lake, will shift to a mixed-evergreen forest (*Lenihan et al.*, 2008). Additionally, rising CO_2 levels have been forecast to cause an increase in forest net primary productivity, but this has yet to be seen (*Lenihan et al.*, 2008).

Although not an exact analogue for future conditions, paleoecological records help reduce uncertainty around many predictions (*IPCC*, 2007; *Swetnam et al.*, 1999). Rising temperatures suggest the possibility of a return to early-Holocene conditions;

however, the comparison is complicated by changing precipitation patterns, higher CO_2 levels, and especially differences in seasonality between the early Holocene and the future. The Hobart Lake record suggests that such changes will favor increased fire activity and an expansion of fire-tolerant and drought-adapted species, including *Pinus ponderosa*, *Quercus garryana*, *Pseudotsuga menziesii*, *Juniperus occidentalis,* and *Calocedrus decurrens*. Species poorly adapted to drought and fire, such as *Abies*, will likely become less abundant due to increased moisture stress and fire activity. Many southwestern Oregon and northern California species are already at their biogeographic limits in the southern Cascade Range. For example, *Juniperus occidentalis* is at its western distributional limit and *Pseudotsuga menziesii*, *Acer macrophyllum*, and *Quercus garryana* are at their eastern limits (*Thompson et al.*, 1999; *U.S. Geological Survey*, 2006). Anticipated climate warming will likely force changes in their distributions in many areas. *Juniperus occidentalis* may be able to expand westward while genera such as *Abies* would likely move upslope or become confined to coastal settings. *Pseudotsuga menziesii* and *Quercus garryana* would likely be able to expand upslope. As the future unfolds, the Hobart Lake paleoecological record provides one more piece of information on which to anticipate future vegetation and fire conditions in the southern Cascade Range.

REFERENCES

Agee, J. K. (1993), *Fire Ecology of Pacific Northwest Forests*, 493 pp., Island Press, Washington, D.C. .

Alley, R. B. (2000), *The Two-Mile Time Machine*, Princeton University Press, Princeton, NJ.

Barron, J. A., L. Heusser, T. Herbert, and M. Lyle (2003), High-resolution climate evolution of coastal northern California during the past 16,000 years *Paleoceanography*, *18*, 1020-1029.

Bartlein, P. J., K. H. Anderson, P. M. Anderson, M. E. Edwards, C. J. Mock, R. S. Thompson, R. S. Webb, and C. Whitlock (1998), Paleoclimate simulations for North America over the past 21,000 years: Features of the simulated climate and comparisons with paleoenvironmental data, *Quaternary Sci Rev*, *17*(6-7), 549-585.

Bennett, K.D., Willis, K.J., 2001. Pollen. In: Smol, J.P., Birks, H.J.B., Last, W.M. (Eds.), Tracking Environmental Change Using Lake Sediments. : Terrestrial, Algal, and Siliceous Indicators, 3. Kluwer Academic Publishers, Dordrecht, pp. 5–32.

Berger, A. L. (1978), Long-term variations of caloric insolation resulting from Earth's orbitalelements, *Quaternary Research*, *9*, 139-167.

Blaauw, M. (2010), Methods and code for 'classical' age-modelling of radiocarbon sequences, *Quaternary Geochronology 5*, 512-518.

Briles, C., C. Whitlock, and P. J. Bartlein (2005), Postglacial vegetation, fire, and climate history of the Siskiyou Mountains, Oregon, USA, *Quaternary Research*, *64*(1), 44-56.

Briles, C., C. Whitlock, P. J. Bartlein, and P. Higuera (2008), Regional and local controls on postglacial vegetation and fire in the Siskiyou Mountains, northern California, USA, *Palaeogeography, Palaeoclimatology, Palaeoecology*, *265*(1-2), 159-169.

Briles, C., C. Whitlock, C. N. Skinner, and J. Mohr (2011), Holocene forest development and maintenance on different substrates in the Klamath Mountains, northern California, USA, *Ecology*, *92*(3), 590-601.

Burns, R., and B. Honkala (1990), *Silvics of North America*, 675 pp., U.S. Department of Agriculture, Forest Service, Washington, DC.

Cayan, A. Luers, G. Franco, and B. Croes (2006), Climate Change Scenarios for California: An Overview, *California Energy Commission PIER working paper*.

COHMAP, M. (1988), Climatic Changes of the Last 18,000 Years: Observations and Model Simulations, *Science*, *241*, 1043-1052.

Cook, E., C. Woodhouse, C. M. Eakin, D. Meko, and D. Stahle (2004), Long-Term Aridity Changes in the Western United States, *Science*, *306*, 1015-1018.

Daly, C., G. Taylor, and J. Aiken (2000), Average Annual Precipitation, Pacific Northwest, 1961-1990, edited, Oregon State University.

Daniels, M. L., R. S. Anderson, and C. Whitlock (2005), Vegetation and fire history since the Late Pleistocene from the Trinity Mountains, northwestern California, USA, *Holocene*, *15*(7), 1062-1071.

Dean Jr., W. (1974), Determination of carbonate and organic matter in calcareous sediments and sedimentary rocks by loss on ignition: comparison with other methods, *J Sediment Petrol*, *44*(No. 1), 242-248.

Dearing, J. (1999), *Environmental Magnetic Susceptibility: Using the Bartington MS2 System*, Chi Publishing, Kenilworth, England.

Diffenbaugh, N. (2003), Global and Regional Controls on Holocene Environments, 116 pp, University of California Santa Cruz.

Faegri, K., and J. Iversen (1975), *Textbook of Pollen Analysis*, Third ed., Hafner Press, New York.

Franklin, J. F., and C. T. Dyrness (1988), Natural Vegetation of Oregon and Washington*Rep.*, Oregon State University Press, Oregon State University, Corvallis, Oregon.

Gedye, S. J., R. T. Jones, W. Tinner, B. Ammann, and F. Oldfield (2000), The use of mineral magnetism in the reconstruction of fire history: a case study from Lago di Origlio, Swiss Alps, *Palaeogeogr Palaeocl*, *164*, 101-110.

Grigg, L. D., and C. Whitlock (1998), Late-Glacial Vegetation and Climate Change in Western Oregon, *Quaternary Research*, *49*, 287-298.

Grimm, E. C. (1987), CONISS: a Fortran 77 program for stratigraphically constrained cluster analysis by the method of incremental sum of squares, *Computers & Geosciences*, *13*(No. 1), 13-35.

Guard, B. J. (1995), *Wetland Plants of Oregon and Washington*, Lone Pine Publishing, Redmond, Washington.

Higuera, P., L. B. Brubaker, P. M. Anderson, F. S. Hu, and T. A. Brown (2009), Vegetation Mediated the Impacts of Postglacial Climate Change on Fire Regimes in the South-Central Brooks Range, Alaska, *Ecol Monogr*, *79*(2), 201-219.

IPCC (2007), Contribution of Working Group I to the Fourth Assessment Report of the Intergovernmental Panel on Climate Change, 2007*Rep.*, Intergovernmental Panel on Climate Change, Cambridge, United Kingdom and New York, NY, USA.

Kapp, R., O. Davis, and J. King (2000), *Pollen and Spores*, Second ed., American Association of Stratigraphic Palynologist Foundation, College Station, Texas.

Lake, F. K. (2013), Historical and cultural fires, tribal management and research issue in Northern California: Trails, fires and tribulations, *Occasion: Interdisciplinary Studies in the Humanities*, *5*, 22.

Lenihan, J., D. Bachelet, R. Neilson, and R. Drapek (2008), Response of vegetation distribution, ecosystem productivity, and fire to climate change scenarios for California, *Climatic Change*, *87*(1), 215-230.

Leung, L., Y. Qian, X. Bian, W. Washington, J. Han, and J. Roads (2004), Mid-Century Ensemble Regional Climate Change Scenarios for the Western United States, *Climatic Change*, *62*(1-3), 75-113.

Lyford, M. E., S. T. Jackson, J. L. Betancourt, and S. T. Gray (2003), Influence of landscape structure and climate variability on a late Holocene plant migration, *Ecol Monogr*, *73*(4), 567-583.

Lyle, M., L. Heusser, C. Ravelo, M. Yamamoto, J. Barron, N. Diffenbaugh, T. Herbert, and D. Andreasen (2012), Out of the Tropics: The Pacific, Great Basin Lakes, and Late Pleistocene Water Cycle in the Western United States, *Science*, *337*.

Mann, M. E., Z. Zhang, S. Rutherford, R. Bradley, M. Hughes, D. Shindell, C. Ammann, G. Faluvegi, and F. Ni (2009), Global Signatures and Dynamical Origins of the Little Ice Age and Medieval Climate Anomaly, *Science*, *326*, 5.

McAndrews, J., A. Berti, and G. Norris (1973), *Key to the Quaternary Pollen and Spores of the Great Lakes Region*, 61 pp., Royal Ontario Museum, Life Sciences, Toronto, Canada.

Minckley, and C. Whitlock (2000), Spatial variation of modern pollen in Oregon and southern Washington, USA, *Reviews of Palaeobotany and Palynology*, *112*, 97-123.

Minckley, T., C. Whitlock, and P. J. Bartlein (2007), Vegetation, fire, and climate history of the northwestern Great Basin during the last 14,000 years, *Quaternary Sci Rev*, *26*(17-18), 2167-2184.

Minore, D. (1979), *Comparative Autecological Characteristics of Northwestern Tree Species: A Literature Review*, 72 pp., Pacific Northwest Forest and Range Experiment Station, U.S. Department of Agriculture, Forest Service, Portland, OR.

Mock, C. J. (1996), Climatic controls and spatial variations of precipitation in the western United States., *Journal of Climate*, *9*, 1111-1125.

Mock, C. J., and A. Brunelle-Daines (1999), A modern analogue of western United States summer palaeoclimate at 6000 years before present, *The Holocene*, *9*(5), 541-545.

Mohr, J. A., C. Whitlock, and C. N. Skinner (2000), Postglacial vegetation and fire history, eastern Klamath Mountains, California, USA, *Holocene*, *10*(5), 587-601.

Mote, P., and E. Salathé Jr (2010), Future Climate of the Pacific Northwest, *Climatic Change*, *102*(1), 29-50.

Odion, D., and D. Sarr (2007), Managing disturbance regimes to maintain biological diversity in forested ecosystems of the Pacific Northwest, *Forest Ecol Manag*, *246*, 57-65.

Oregon Department of Forestry, S. o. O. (2013), 2013: An epic fire season in Oregon, edited, State of Oregon, http://www.oregon.gov/ODF/Pages/index.aspx.
PRISM Climate Group (2014), edited, Oregon State University.

Reimer, P. J., et al. (2009), IntCal09 and Marine09 radiocarbon age calibration curves, 0-50,000 years cal BP, *Radiocarbon*, *51*, 1111-1150.

Sea, D. S., and C. Whitlock (1995), Postglacial Vegetation and Climate of the Cascade Range, Central Oregon, *Quaternary Research*, *43*(3), 370-381.

Skinner, A. H. Taylor, and J. K. Agee (2006), *Klamath Mountains bioregion*, University of California Press, Berkeley.

Stuiver, M., P. J. Reimer, and R. W. Reimer (2010), CALIB 6.0, edited.
Swetnam, T. W., C. D. Allen, and J. L. Betancourt (1999), Applied Historical Ecology: Using the Past to Manage for the Future, *Ecol Appl*, *9*(4), 1189-1206.

The Nature Conservancy (1988), Hobart Lake Study*Rep.*, 68 pp, The Nature Conservancy

Oregon Natural Heritage Program, Unpublished Report in colaboration with Oregon Natural Heritage Program.

Thompson, R. S., K. H. Anderson, and P. Bartlein (1999), Atlas of Relations Between Climatic Parameters and Distributions of Important Trees and Shrubs in North America*Rep.*, U.S. Geological Survey.

Thompson, R. S., C. Whitlock, P. J. Bartlein, S. P. Harrison, and W. G. Spaulding (1993), Climatic changes in western United States since 18,000 yr BP, in *Global Climates since the Last Glacial Maximum*, edited by H. E. Wright Jr., J. E. Kutzbach, T. Webb III, W. F. Ruddiman, F. A. Street-Perrott and P. Bartlein, pp. 468-513, University of Minnesota Press, Minneapolis.

U.S. Geological Survey (2006), Digital Representations of Tree Species Range Maps from "Atlas of United States Trees" by Elbert L. Little, Jr. (and other publications), edited, USGS, http://esp.cr.usgs.gov/data/atlas/little/.

Vacco, D. A., P. U. Clark, A. C. Mix, H. Cheng, and R. L. Edward (2005), A speleothem record of Younger Dryas cooling, Klamath Mountains, Oregon, USA, *Quaternary Research*, *64*(2), 249-256.

Walsh, M. K., C. Whitlock, and P. J. Bartlein (2010), 1200 years of fire and vegetation history in the Willamette Valley, Oregon and Washington, reconstructed using high-resolution macroscopic charcoal and pollen analysis, *Palaeogeogr Palaeocl*, *297*(2), 273-289.

Westerling, A. L., B. P. Bryant, H. K. Preisler, T. P. Holmes, H. G. Hidalgo, T. Das, and S. R. Shrestha (2011), Climate change and growth scenarios for California wildfire, *Climatic Change*, *109*(1), 445-463.

Western Ecology Division, E., Environmental Protection Agency (2011), Ecoregions of North America.

Western Regional Climate Center, D. R. I. (2013), Climate of Oregon, edited.

Whitlock, Cathy and C. Larsen (2001), Charcoal as a fire proxy, in *Tracking environmental change using lake sediments*, edited by H. J. B. B. J.P. Smol, W.M. Last, pp. 74-97, Kluwer Academic Publishers, Dordrecht, Netherlands.

Whitlock, Cathy and R. S. Anderson (2003), *Fire history reconstructions based on sediment records from lakes and wetlands*, Springer-Verlag, New York.

Whitlock, C. N. Skinner, P. J. Bartlein, T. Minckley, and J. A. Mohr (2004), Comparison of charcoal and tree-ring records of recent fires in the eastern Klamath Mountains, California, USA, *Can J Forest Res*, *34*(10), 2110-2121.

Whittaker, R. H. (1960), Vegetation of the Siskiyou Mountains, Oregon and California, *Ecol Monogr*, *30*(3), 280-338.

Whittaker, R. H. (1972), Evolution and Measurement of Species Diversity, *Taxon*, *21*(2/3), 213-251.

Worona, M. A., and C. Whitlock (1995), Late Quaternary vegetation and climate history near Little Lake, central Coast Range, Oregon, *GSA Bulletin*, *107*(7), 867-876.

Zdanowicz, C. M., G. A. Zielinski, and M. S. Germani (1999), Mount Mazama eruption: Calendrical age verified and atmospheric impact assessed, *Geology*, *27*(7), 621-624.

APPENDICES

APPENDIX A

RAW CHARCOAL COUNTS

Age (cal yr BP)	Sediment Depth (cm)	Charcoal Counts (# particles)	Sediment Volume (cm^3)
-63	0	0	2
-58	1	3	2
-53	2	1	2
-48	3	1	2
-43	4	6	2
-38	5	6	2
-33	6	7	2
-29	7	11	2
-24	8	11	2
-19	9	7	2
-14	10	4	2
-9	11	5	2
-4	12	8	2
1	13	5	2
6	14	16	2
11	15	7	2
16	16	4	2
21	17	11	2
26	18	7	2
31	19	5	2
35	20	4	2
40	21	1	2
45	22	4	2
50	23	4	2
55	24	2	2
60	25	2	2
65	26	4	2
70	27	7	2
74	28	2	2
79	29	1	2
84	30	0	2
89	31	0	2
94	32	7	2

Age (cal yr BP)	Sediment Depth (cm)	Charcoal Counts (# particles)	Sediment Volume (cm^3)
99	33	1	2
103	34	1	2
108	35	0	2
113	36	4	2
118	37	4	2
122	38	0	2
127	39	2	2
132	40	2	2
137	41	6	2
141	42	0	2
146	43	8	2
151	44	0	2
155	45	6	2
160	46	8	2
165	47	1	2
169	48	6	2
174	49	3	2
179	50	1	2
183	51	5	2
188	52	3	2
193	53	2	2
197	54	10	2
202	55	3	2
206	56	4	2
211	57	4	2
215	58	1	2
220	59	1	2
224	60	5	2
229	61	6	2
233	62	13	2
238	63	3	2
242	64	7	2
246	65	6	2
251	66	6	2
255	67	5	2
260	68	5	2

Age (cal yr BP)	Sediment Depth (cm)	Charcoal Counts (# particles)	Sediment Volume (cm^3)
264	69	5	2
268	70	5	2
272	71	4	2
277	72	5	2
281	73	7	2
285	74	6	2
289	75	7	2
294	76	1	2
298	77	9	2
302	78	18	2
306	79	5	2
310	80	9	2
314	81	5	2
318	82	9	2
323	83	10	2
327	84	10	2
331	85	7	2
335	86	10	2
339	87	3	2
343	88	13	2
346	89	5	2
350	90	9	2
354	91	6	2
358	92	7	2
362	93	15	2
366	94	3	2
369	95	8	2
373	96	9	2
377	97	13	2
381	98	28	2
384	99	35	2
388	100	43	2
392	101	59	2
395	102	10	2
399	103	2	2
402	104	6	2

Age (cal yr BP)	Sediment Depth (cm)	Charcoal Counts (# particles)	Sediment Volume (cm^3)
406	105	11	2
409	106	4	2
413	107	9	2
416	108	2	2
420	109	2	2
423	110	12	2
426	111	19	2
430	112	13	2
433	113	26	2
436	114	0	2
440	115	9	2
443	116	7	2
446	117	4	2
449	118	12	2
452	119	18	2
455	120	2	2
458	121	0	2
461	122	0	2
464	123	0	2
467	124	0	2
470	125	0	2
473	126	0	2
476	127	0	2
479	128	11	2
482	129	16	2
484	130	17	2
487	131	7	2
490	132	23	2
492	133	8	2
495	134	2	2
498	135	8	2
500	136	9	2
503	137	2	2
505	138	10	2
508	139	16	2
510	140	23	2

Age (cal yr BP)	Sediment Depth (cm)	Charcoal Counts (# particles)	Sediment Volume (cm^3)
512	141	9	2
515	142	7	2
517	143	10	2
519	144	8	2
522	145	13	2
524	146	14	2
526	147	14	2
528	148	2	2
530	149	35	2
532	150	8	2
534	151	14	2
536	152	2	2
538	153	3	2
540	154	3	2
542	155	9	2
543	156	6	2
545	157	9	2
547	158	8	2
549	159	3	2
550	160	2	2
552	161	3	2
554	162	12	2
556	163	68	2
557	164	11	2
559	165	1	2
561	166	7	2
563	167	6	2
565	168	8	2
566	169	10	2
568	170	3	2
570	171	4	2
572	172	6	2
575	173	13	2
577	174	16	2
579	175	10	2

Age (cal yr BP)	Sediment Depth (cm)	Charcoal Counts (# particles)	Sediment Volume (cm^3)
581	176	4	2
584	177	3	2
586	178	5	2
588	179	5	2
591	180	8	2
594	181	17	2
597	182	20	2
600	183	18	2
603	184	10	2
606	185	16	2
609	186	40	2
613	187	25	2
616	188	9	2
620	189	26	2
624	190	25	2
628	191	17	2
632	192	10	2
636	193	20	2
641	194	6	2
645	195	4	2
650	196	5	2
655	197	10	2
660	198	15	2
665	199	15	2
670	200	23	2
676	201	19	2
682	202	17	2
687	203	32	2
693	204	12	2
699	205	22	2
705	206	40	2
712	207	7	2
718	208	3	2
724	209	12	2
731	210	12	2
738	211	7	2

Age (cal yr BP)	Sediment Depth (cm)	Charcoal Counts (# particles)	Sediment Volume (cm^3)
744	212	12	2
751	213	10	2
758	214	10	2
765	215	14	2
773	216	8	2
780	217	1	2
787	218	9	2
795	219	13	2
802	220	14	2
810	221	19	2
818	222	7	2
825	223	7	2
833	224	9	2
841	225	17	2
849	226	12	2
857	227	15	2
865	228	11	2
873	229	13	2
882	230	16	2
890	231	13	2
898	232	15	2
906	233	11	2
915	234	11	2
923	235	21	2
923	230	48	2
928	231	43	2
932	232	38	2
937	233	30	2
942	234	28	2
946	235	28	2
951	236	22	2
956	237	37	2
960	238	17	2
965	239	27	2
970	240	18	2
975	241	27	2

Age (cal yr BP)	Sediment Depth (cm)	Charcoal Counts (# particles)	Sediment Volume (cm^3)
979	242	56	2
984	243	54	2
989	244	12	2
994	245	21	2
999	246	17	2
1003	247	49	2
1008	248	82	2
1013	249	48	2
1018	250	41	2
1023	251	28	2
1028	252	18	2
1033	253	24	2
1038	254	18	2
1042	255	20	2
1047	256	8	2
1052	257	21	2
1057	258	28	2
1062	259	32	2
1067	260	20	2
1072	261	23	2
1077	262	19	2
1082	263	19	2
1087	264	28	2
1092	265	23	2
1097	266	30	2
1102	267	26	2
1107	268	34	2
1112	269	33	2
1117	270	18	2
1123	271	12	2
1128	272	22	2
1133	273	36	2
1138	274	18	2
1143	275	17	2
1148	276	21	2
1153	277	11	2

Age (cal yr BP)	Sediment Depth (cm)	Charcoal Counts (# particles)	Sediment Volume (cm^3)
1158	278	10	2
1164	279	18	2
1169	280	27	2
1174	281	18	2
1179	282	23	2
1184	283	19	2
1190	284	16	2
1195	285	23	2
1200	286	18	2
1205	287	21	2
1211	288	24	2
1216	289	54	2
1221	290	29	2
1227	291	34	2
1232	292	30	2
1237	293	31	2
1243	294	23	2
1248	295	35	2
1253	296	33	2
1259	297	33	2
1264	298	37	2
1269	299	31	2
1275	300	19	2
1280	301	14	2
1286	302	26	2
1291	303	34	2
1297	304	31	2
1302	305	22	2
1307	306	19	2
1313	307	31	2
1318	308	18	2
1324	309	23	2
1329	310	19	2
1335	311	9	2
1340	312	16	2
1346	313	13	2

Age (cal yr BP)	Sediment Depth (cm)	Charcoal Counts (# particles)	Sediment Volume (cm^3)
1351	314	16	2
1357	315	12	2
1363	316	4	2
1368	317	27	2
1374	318	10	2
1379	319	20	2
1385	320	20	2
1391	321	20	2
1396	322	27	2
1402	323	22	2
1407	324	16	2
1413	325	23	2
1419	326	20	2
1424	327	16	2
1430	328	27	2
1436	329	40	2
1442	330	17	2
1447	331	30	2
1453	332	24	2
1459	333	22	2
1464	334	29	2
1470	335	22	2
1476	336	14	2
1482	337	32	2
1488	338	18	2
1493	339	14	2
1499	340	15	2
1505	341	16	2
1511	342	26	2
1517	343	18	2
1522	344	13	2
1528	345	19	2
1534	346	18	2
1540	347	12	2
1546	348	6	2
1552	349	14	2

Age (cal yr BP)	Sediment Depth (cm)	Charcoal Counts (# particles)	Sediment Volume (cm^3)
1558	350	6	2
1564	351	10	2
1570	352	3	2
1576	353	18	2
1581	354	15	2
1587	355	9	2
1593	356	6	2
1599	357	23	2
1605	358	16	2
1611	359	10	2
1617	360	21	2
1623	361	21	2
1629	362	24	2
1635	363	24	2
1641	364	15	2
1647	365	25	2
1653	366	39	2
1660	367	26	2
1666	368	20	2
1672	369	20	2
1678	370	22	2
1684	371	30	2
1690	372	26	2
1696	373	22	2
1702	374	23	2
1708	375	23	2
1714	376	35	2
1721	377	20	2
1727	378	46	2
1733	379	28	2
1739	380	40	2
1745	381	41	2
1752	382	34	2
1758	383	48	2
1764	384	44	2

Age (cal yr BP)	Sediment Depth (cm)	Charcoal Counts (# particles)	Sediment Volume (cm^3)
1770	385	36	2
1776	386	27	2
1783	387	38	2
1789	388	26	2
1795	389	26	2
1801	390	25	2
1808	391	23	2
1814	392	36	2
1820	393	31	2
1827	394	66	2
1833	395	38	2
1839	396	28	2
1846	397	31	2
1852	398	52	2
1858	399	24	2
1865	400	26	2
1871	401	15	2
1877	402	24	2
1884	403	31	2
1890	404	14	2
1897	405	32	2
1903	406	21	2
1909	407	29	2
1916	408	14	2
1922	409	13	2
1929	410	17	2
1935	411	23	2
1942	412	20	2
1948	413	22	2
1955	414	17	2
1961	415	21	2
1968	416	11	2
1974	417	20	2
1981	418	16	2
1987	419	31	2
1994	420	24	2

Age (cal yr BP)	Sediment Depth (cm)	Charcoal Counts (# particles)	Sediment Volume (cm^3)
2000	421	38	2
2007	422	15	2
2013	423	11	2
2020	424	18	2
2026	425	27	2
2033	426	12	2
2040	427	33	2
2046	428	13	2
2053	429	15	2
2059	430	15	2
2066	431	30	2
2073	432	23	2
2079	433	22	2
2086	434	43	2
2093	435	35	2
2099	436	24	2
2106	437	22	2
2113	438	23	2
2119	439	22	2
2126	440	19	2
2133	441	18	2
2139	442	21	2
2146	443	18	2
2153	444	14	2
2160	445	12	2
2166	446	5	2
2173	447	1	2
2180	448	9	2
2187	449	25	2
2193	450	18	2
2200	451	29	2
2207	452	20	2
2214	453	71	2
2221	454	40	2
2227	455	47	2
2234	456	50	2

Age (cal yr BP)	Sediment Depth (cm)	Charcoal Counts (# particles)	Sediment Volume (cm^3)
2241	457	24	2
2248	458	14	2
2255	459	32	2
2262	460	23	2
2268	461	12	2
2275	462	16	2
2282	463	42	2
2289	464	9	2
2296	465	23	2
2303	466	38	2
2310	467	24	2
2317	468	24	2
2324	469	33	2
2331	470	11	2
2337	471	22	2
2344	472	18	2
2351	473	26	2
2358	474	47	2
2365	475	47	2
2372	476	12	2
2379	477	47	2
2386	478	32	2
2393	479	35	2
2400	480	28	2
2407	481	36	2
2414	482	21	2
2421	483	20	2
2428	484	41	2
2435	485	36	2
2442	486	38	2
2450	487	29	2
2457	488	41	2
2464	489	37	2
2471	490	28	2
2478	491	42	2
2485	492	33	2

Age (cal yr BP)	Sediment Depth (cm)	Charcoal Counts (# particles)	Sediment Volume (cm^3)
2492	493	0	2
2499	494	0	2
2506	495	0	2
2513	496	0	2
2520	497	0	2
2528	498	0	2
2535	499	0	2
2542	500	35	2
2549	501	31	2
2556	502	33	2
2563	503	32	2
2571	504	34	2
2578	505	31	2
2585	506	37	2
2592	507	13	2
2599	508	54	2
2607	509	36	2
2614	510	48	2
2621	511	26	2
2628	512	42	2
2635	513	21	2
2643	514	38	2
2650	515	28	2
2657	516	31	2
2664	517	53	2
2672	518	68	2
2679	519	30	2
2686	520	33	2
2694	521	23	2
2701	522	30	2
2708	523	33	2
2715	524	43	2
2723	525	37	2
2730	526	41	2
2737	527	20	2

Age (cal yr BP)	Sediment Depth (cm)	Charcoal Counts (# particles)	Sediment Volume (cm^3)
2745	528	47	2
2752	529	51	2
2759	530	36	2
2767	531	46	2
2774	532	61	2
2782	533	39	2
2789	534	28	2
2796	535	20	2
2804	536	15	2
2811	537	33	2
2819	538	34	2
2826	539	45	2
2833	540	59	2
2841	541	40	2
2848	542	45	2
2856	543	46	2
2863	544	25	2
2871	545	38	2
2878	546	15	2
2885	547	38	2
2893	548	47	2
2900	549	33	2
2908	550	34	2
2915	551	35	2
2923	552	33	2
2930	553	23	2
2938	554	62	2
2945	555	51	2
2953	556	39	2
2960	557	38	2
2968	558	15	2
2975	559	33	2
2983	560	33	2
2990	561	35	2
2998	562	25	2
3006	563	29	2

Age (cal yr BP)	Sediment Depth (cm)	Charcoal Counts (# particles)	Sediment Volume (cm^3)
3013	564	20	2
3021	565	26	2
3028	566	38	2
3036	567	46	2
3043	568	17	2
3051	569	44	2
3059	570	57	2
3066	571	33	2
3074	572	41	2
3081	573	33	2
3089	574	32	2
3097	575	30	2
3104	576	23	2
3112	577	15	2
3120	578	31	2
3127	579	30	2
3135	580	21	2
3143	581	41	2
3150	582	44	2
3158	583	40	2
3166	584	29	2
3173	585	46	2
3181	586	37	2
3189	587	24	2
3196	588	37	2
3204	589	12	2
3212	590	23	2
3219	591	35	2
3227	592	38	2
3235	593	24	2
3243	594	27	2
3250	595	50	2
3258	596	50	2
3266	597	33	2
3274	598	48	2
3281	599	42	2

Age (cal yr BP)	Sediment Depth (cm)	Charcoal Counts (# particles)	Sediment Volume (cm^3)
3289	600	26	2
3297	601	27	2
3305	602	49	2
3312	603	83	2
3320	604	50	2
3328	605	24	2
3336	606	49	2
3344	607	47	2
3351	608	20	2
3359	609	43	2
3367	610	16	2
3375	611	15	2
3383	612	31	2
3391	613	31	2
3398	614	26	2
3406	615	24	2
3414	616	22	2
3422	617	34	2
3430	618	22	2
3438	619	40	2
3446	620	50	2
3453	621	55	2
3461	622	21	2
3469	623	23	2
3477	624	81	2
3485	625	60	2
3493	626	12	2
3501	627	22	2
3509	628	40	2
3517	629	51	2
3525	630	19	2
3532	631	29	2
3540	632	29	2
3548	633	96	2
3556	634	50	2
3564	635	56	2

Age (cal yr BP)	Sediment Depth (cm)	Charcoal Counts (# particles)	Sediment Volume (cm^3)
3572	636	66	2
3580	637	49	2
3588	638	56	2
3596	639	87	2
3604	640	60	2
3612	641	43	2
3620	642	29	2
3628	643	52	2
3636	644	64	2
3644	645	51	2
3652	646	78	2
3660	647	50	2
3668	648	77	2
3676	649	86	2
3684	650	44	2
3692	651	28	2
3700	652	39	2
3708	653	35	2
3716	654	35	2
3724	655	29	2
3732	656	43	2
3740	657	60	2
3748	658	59	2
3756	659	46	2
3765	660	67	2
3773	661	53	2
3781	662	70	2
3789	663	42	2
3797	664	30	2
3805	665	28	2
3813	666	32	2
3821	667	30	2
3829	668	45	2
3837	669	23	2
3845	670	18	2
3854	671	70	2

Age (cal yr BP)	Sediment Depth (cm)	Charcoal Counts (# particles)	Sediment Volume (cm^3)
3862	672	37	2
3870	673	23	2
3878	674	38	2
3886	675	14	2
3894	676	18	2
3902	677	12	2
3911	678	28	2
3919	679	23	2
3927	680	34	2
3935	681	41	2
3943	682	45	2
3951	683	21	2
3960	684	24	2
3968	685	38	2
3976	686	47	2
3984	687	32	2
3992	688	27	2
4000	689	52	2
4009	690	15	2
4017	691	48	2
4025	692	20	2
4033	693	29	2
4042	694	0	2
4050	695	0	2
4058	696	0	2
4066	697	0	2
4074	698	0	2
4083	699	0	2
4091	700	42	2
4099	701	43	2
4107	702	47	2
4116	703	54	2
4124	704	43	2
4132	705	38	2
4140	706	50	2
4149	707	47	2

Age (cal yr BP)	Sediment Depth (cm)	Charcoal Counts (# particles)	Sediment Volume (cm^3)
4157	708	44	2
4165	709	26	2
4174	710	52	2
4182	711	69	2
4190	712	33	2
4198	713	49	2
4207	714	54	2
4215	715	48	2
4223	716	46	2
4232	717	36	2
4240	718	26	2
4248	719	223	2
4257	720	33	2
4265	721	40	2
4273	722	48	2
4282	723	26	2
4290	724	42	2
4298	725	5	2
4307	726	31	2
4315	727	34	2
4323	728	13	2
4332	729	57	2
4340	730	80	2
4348	731	54	2
4357	732	55	2
4365	733	60	2
4374	734	72	2
4382	735	47	2
4390	736	83	2
4399	737	127	2
4407	738	107	2
4416	739	103	2
4424	740	65	2
4432	741	52	2
4441	742	40	2
4449	743	44	2

Age (cal yr BP)	Sediment Depth (cm)	Charcoal Counts (# particles)	Sediment Volume (cm^3)
4458	744	49	2
4466	745	21	2
4474	746	39	2
4483	747	28	2
4491	748	46	2
4500	749	27	2
4508	750	36	2
4517	751	44	2
4525	752	30	2
4533	753	50	2
4542	754	43	2
4550	755	28	2
4559	756	60	2
4567	757	35	2
4576	758	70	2
4584	759	20	2
4593	760	28	2
4601	761	48	2
4610	762	38	2
4618	763	36	2
4627	764	23	2
4635	765	77	2
4643	766	65	2
4652	767	29	2
4660	768	26	2
4669	769	72	2
4677	770	70	2
4686	771	11	2
4694	772	50	2
4703	773	29	2
4712	774	32	2
4720	775	21	2
4729	776	33	2
4737	777	24	2
4746	778	29	2

Age (cal yr BP)	Sediment Depth (cm)	Charcoal Counts (# particles)	Sediment Volume (cm^3)
4754	779	46	2
4763	780	10	2
4771	781	9	2
4780	782	45	2
4788	783	43	2
4797	784	27	2
4805	785	38	2
4814	786	26	2
4823	787	35	2
4831	788	25	2
4840	789	23	2
4848	790	46	2
4857	791	3	2
4865	792	0	2
4874	793	4	2
4883	794	0	2
4891	795	0	2
4900	796	0	2
4908	797	0	2
4917	798	0	2
4925	799	0	2
4934	800	42	2
4943	801	31	2
4951	802	56	2
4960	803	36	2
4969	804	28	2
4977	805	35	2
4986	806	23	2
4994	807	37	2
5003	808	68	2
5012	809	35	2
5020	810	35	2
5029	811	40	2
5038	812	50	2
5046	813	21	2
5055	814	36	2

Age (cal yr BP)	Sediment Depth (cm)	Charcoal Counts (# particles)	Sediment Volume (cm^3)
5063	815	34	2
5072	816	19	2
5081	817	28	2
5089	818	313	2
5098	819	40	2
5107	820	34	2
5115	821	31	2
5124	822	29	2
5133	823	18	2
5141	824	18	2
5150	825	41	2
5159	826	27	2
5168	827	43	2
5176	828	30	2
5185	829	180	2
5194	830	69	2
5202	831	11	2
5211	832	68	2
5220	833	49	2
5228	834	18	2
5237	835	31	2
5246	836	24	2
5255	837	49	2
5263	838	76	2
5272	839	114	2
5281	840	20	2
5289	841	152	2
5298	842	100	2
5307	843	33	2
5316	844	52	2
5324	845	32	2
5333	846	6	2
5342	847	21	2
5351	848	18	2
5359	849	21	2
5368	850	26	2

Age (cal yr BP)	Sediment Depth (cm)	Charcoal Counts (# particles)	Sediment Volume (cm^3)
5377	851	23	2
5386	852	40	2
5394	853	55	2
5403	854	13	2
5412	855	22	2
5421	856	28	2
5429	857	60	2
5438	858	36	2
5447	859	38	2
5456	860	30	2
5465	861	34	2
5473	862	23	2
5482	863	30	2
5491	864	40	2
5500	865	41	2
5509	866	41	2
5517	867	45	2
5526	868	59	2
5535	869	27	2
5544	870	19	2
5553	871	17	2
5561	872	13	2
5570	873	20	2
5579	874	23	2
5588	875	32	2
5597	876	17	2
5606	877	37	2
5614	878	76	2
5623	879	31	2
5632	880	25	2
5641	881	28	2
5650	882	44	2
5659	883	36	2
5667	884	31	2
5676	885	19	2
5685	886	32	2

Age (cal yr BP)	Sediment Depth (cm)	Charcoal Counts (# particles)	Sediment Volume (cm^3)
5694	887	18	2
5703	888	30	2
5712	889	53	2
5721	890	97	2
5729	891	82	2
5738	892	57	2
5747	893	6	2
5756	894	6	2
5765	895	23	2
5774	896	144	2
5783	897	46	2
5791	898	0	2
5800	899	0	2
5809	900	40	2
5818	901	44	2
5827	902	39	2
5836	903	14	2
5845	904	14	2
5854	905	58	2
5863	906	88	2
5871	907	41	2
5880	908	44	2
5889	909	81	2
5898	910	60	2
5907	911	19	2
5916	912	10	2
5925	913	57	2
5934	914	43	2
5943	915	48	2
5952	916	67	2
5961	917	50	2
5969	918	34	2
5978	919	27	2
5987	920	65	2
5996	921	52	2
6005	922	73	2

Age (cal yr BP)	Sediment Depth (cm)	Charcoal Counts (# particles)	Sediment Volume (cm^3)
6014	923	40	2
6023	924	58	2
6032	925	27	2
6041	926	59	2
6050	927	65	2
6059	928	27	2
6068	929	30	2
6077	930	47	2
6086	931	24	2
6094	932	26	2
6103	933	37	2
6112	934	48	2
6121	935	52	2
6130	936	40	2
6139	937	51	2
6148	938	63	2
6157	939	86	2
6166	940	66	2
6175	941	58	2
6184	942	35	2
6193	943	42	2
6202	944	30	2
6211	945	22	2
6220	946	23	2
6229	947	2	2
6238	948	81	2
6247	949	56	2
6256	950	72	2
6265	951	89	2
6274	952	126	2
6283	953	59	2
6292	954	351	2
6301	955	40	2
6310	956	31	2
6318	957	86	2
6327	958	28	2

Age (cal yr BP)	Sediment Depth (cm)	Charcoal Counts (# particles)	Sediment Volume (cm^3)
6336	959	14	2
6345	960	75	2
6354	961	21	2
6363	962	6	2
6372	963	13	2
6381	964	37	2
6390	965	28	2
6399	966	36	2
6408	967	10	2
6417	968	22	2
6426	969	26	2
6435	970	23	2
6444	971	4	2
6453	972	10	2
6462	973	60	2
6471	974	40	2
6480	975	29	2
6489	976	54	2
6498	977	91	2
6507	978	8	2
6516	979	3	2
6525	980	49	2
6534	981	28	2
6543	982	40	2
6552	983	84	2
6561	984	86	2
6571	985	90	2
6580	986	71	2
6589	987	13	2
6598	988	74	2
6607	989	24	2
6616	990	28	2
6625	991	48	2
6634	992	17	2
6643	993	1	2
6652	994	4	2

Age (cal yr BP)	Sediment Depth (cm)	Charcoal Counts (# particles)	Sediment Volume (cm^3)
6661	995	14	2
6670	996	37	2
6679	997	36	2
6688	998	165	2
6697	999	0	2
6706	1000	42	2
6715	1001	58	2
6724	1002	36	2
6733	1003	67	2
6742	1004	75	2
6751	1005	39	2
6760	1006	140	2
6769	1007	93	2
6778	1008	156	2
6787	1009	33	2
6797	1010	98	2
6806	1011	58	2
6815	1012	82	2
6824	1013	92	2
6833	1014	259	2
6842	1015	54	2
6851	1016	125	2
6860	1017	114	2
6869	1018	49	2
6878	1019	43	2
6887	1020	87	2
6896	1021	41	2
6905	1022	37	2
6914	1023	56	2
6924	1024	35	2
6933	1025	57	2
6942	1026	66	2
6951	1027	99	2
6960	1028	22	2
6969	1029	41	2

Age (cal yr BP)	Sediment Depth (cm)	Charcoal Counts (# particles)	Sediment Volume (cm^3)
6978	1030	46	2
6987	1031	41	2
6996	1032	133	2
7005	1033	60	2
7014	1034	64	2
7024	1035	44	2
7033	1036	241	2
7042	1037	41	2
7051	1038	79	2
7060	1039	56	2
7069	1040	71	2
7078	1041	134	2
7087	1042	63	2
7096	1043	26	2
7105	1044	52	2
7115	1045	88	2
7124	1046	60	2
7133	1047	62	2
7142	1048	84	2
7151	1049	55	2
7160	1050	41	2
7169	1051	49	2
7178	1052	57	2
7187	1053	32	2
7197	1054	25	2
7206	1055	28	2
7215	1056	28	2
7224	1057	29	2
7233	1058	27	2
7242	1059	82	2
7251	1060	60	2
7260	1061	71	2
7270	1062	28	2
7279	1063	59	2
7288	1064	30	2
7297	1065	38	2

Age (cal yr BP)	Sediment Depth (cm)	Charcoal Counts (# particles)	Sediment Volume (cm^3)
7306	1066	45	2
7315	1067	105	2
7324	1068	14	2
7333	1069	54	2
7343	1070	45	2
7352	1071	16	2
7361	1072	29	2
7370	1073	10	2
7379	1074	56	2
7388	1075	47	2
7397	1076	45	2
7407	1077	28	2
7416	1078	62	2
7425	1079	49	2
7434	1080	29	2
7443	1081	30	2
7452	1082	22	2
7461	1083	83	2
7471	1084	40	2
7480	1085	30	2
7489	1086	100	2
7498	1087	53	2
7507	1088	167	2
7516	1089	33	2
7525	1090	18	2
7535	1091	39	2
7544	1092	50	2
7553	1093	2	2
7562	1094	22	2
7571	1095	11	2
7580	1096	11	2
7589	1097	3	2
7599	1098	0	2
7608	1099	0	2
7617	1100	70	2
7626	1101	27	2

Age (cal yr BP)	Sediment Depth (cm)	Charcoal Counts (# particles)	Sediment Volume (cm^3)
7635	1102	90	2
7644	1103	95	2
7654	1104	109	2
7663	1105	92	2
7672	1106	25	2
7681	1107	50	2
7690	1108	63	2
7699	1109	58	2
7708	1110	22	2
7718	1111	22	2
7727	1112	33	2
7736	1113	38	2
7745	1114	20	2
7754	1115	11	2
7763	1116	18	2
7773	1117	74	2
7782	1118	17	2
7791	1119	84	2
7800	1120	19	2
7809	1121	35	2
7818	1122	43	2
7828	1123	76	2
7837	1124	32	2
7846	1125	65	2
7855	1126	76	2
7864	1127	43	2
7873	1128	2	2
7882	1129	20	2
7892	1130	15	2
7901	1131	6	2
7910	1132	19	2
7919	1133	28	2
7928	1134	11	2
7937	1135	38	2
7947	1136	23	2
7956	1137	3	2

Age (cal yr BP)	Sediment Depth (cm)	Charcoal Counts (# particles)	Sediment Volume (cm^3)
7965	1138	66	2
7974	1139	6	2
7983	1140	32	2
7992	1141	67	2
8001	1142	59	2
8011	1143	117	2
8020	1144	71	2
8029	1145	59	2
8038	1146	66	2

APPENDIX B

POLLEN KEY

HP	HALF PINE
H	HAPLOXYLON PINE
E	DIPLOXYLON
P	PINUS
AB	ABIES
HA	HALF ABIES
LX	PSEUDOTSUGA
CU	JUNIPERUS-CUPRESSACEAE
AR	ALNUS RUBRA
AS	ALNUS SINUATA
CY	CORYLUS
S	SALIX
PU	POPULUS UNDIFF
F	FRAXINUS
Q1	QUERCUS EVERGREEN
Q2	QUERCUS DECIDUOUS
AM	ACER MACROPHYLLUM
AC	ACER CIRCINATUM
R3	AMELANCHIER
RS	SPIRAEA
TP	POTENTILLA
CE	CEANOTHUS
CH	CHYRSOLEPIS/LITHOCARPUS
AX	ARCETHOBIUM
SR	SARCOBATUS
G	POACEAE
R	ARTEMISIA
TU	TUBULIFLORAE
LG	LIGULIFLORAE
K	AMARANTHACEAE
UM	UMBELLIFERAE
PC	POLYGONUM CALIFORNICUM
BR	BRASSICACEAE
UR	URTICA
CR	CORNUS
CP	CERCOCARPUS

L	LILLIACEAE
N	NUPHAR
MY	MYRIOPHYLLUM
UP	POTAMOGETON
PS	PEDIASTRUM SIMPLEX
PD	PEDIASTRUM DUPLEX
PA	PEDIASTRUM ARANEOSUM
PB	PEDIASTRUM BORYANUM
PI	PEDIASTRUM INTEGRUM
Y	CYPERACEAE
EQ	EQUISETUM
DR	DRYOPTERUS
TY	TYPHA
PT	PTERIDIUM
LY	LYCOPODIUM

APPENDIX C

RAW POLLEN COUNTS

Depth	Age	HP	H	E	P	AB	HA	LX	CU
4.00	11	17	27	17	73	38	1	33	57
4.16	89	18	16	12	52	20	2	95	35
4.32	165	118	19	2	46	12	5	35	55
4.48	238	72	19	0	66	5	4	82	13
4.64	306	113	16	2	32	15	4	98	7
4.80	369	108	10	0	28	4	4	55	22
4.96	426	114	30	2	42	13	20	78	16
5.19	495	143	11	3	50	13	17	51	15
5.35	532	75	14	2	24	13	7	82	10
5.51	561	117	16	2	32	11	21	97	14
5.67	597	72	9	0	73	38	31	70	11
5.83	660	85	16	1	38	16	18	65	40
5.99	758	97	50	1	36	22	15	39	37
6.02	780	68	27	1	37	12	10	45	59
6.17	898	106	25	4	38	11	13	40	47
6.18	906	79	14	2	49	8	13	51	43
6.33	937	118	32	2	51	28	42	62	22
6.34	942	86	18	3	50	29	23	53	44
6.49	1013	136	23	6	40	11	16	28	61
6.50	1018	51	20	16	61	19	19	56	28
6.66	1097	39	28	7	99	44	23	50	17
6.82	1179	48	17	8	74	20	32	43	19
6.98	1264	45	24	14	64	23	32	39	11
7.14	1351	45	27	12	49	19	21	36	38
7.30	1442	37	22	7	62	19	18	47	30
7.46	1534	32	14	5	52	25	13	36	32
7.62	1629	64	15	2	63	28	43	46	24
7.78	1727	91	22	3	58	20	29	59	23
7.94	1827	115	21	1	70	20	13	46	24
8.10	1929	92	16	1	63	22	32	29	64
8.26	2033	131	30	3	68	16	12	56	21
8.44	2153	79	38	1	60	12	18	49	31
8.60	2262	113	21	1	70	18	17	56	18
8.76	2372	78	27	1	55	22	15	55	30
8.92	2485	137	34	2	79	21	26	51	23
Depth	Age	AR	AS	CY	S	PU	F	Q1	Q2
4.00	11	17	27	17	73	38	1	33	57
4.16	89	18	16	12	52	20	2	95	35
4.32	165	118	19	2	46	12	5	35	55
4.48	238	72	19	0	66	5	4	82	13
4.64	306	113	16	2	32	15	4	98	7
4.80	369	108	10	0	28	4	4	55	22
4.96	426	114	30	2	42	13	20	78	16

5.19	495	143	11	3	50	13	17	51	15
5.35	532	75	14	2	24	13	7	82	10
5.51	561	117	16	2	32	11	21	97	14
5.67	597	72	9	0	73	38	31	70	11
5.83	660	85	16	1	38	16	18	65	40
5.99	758	97	50	1	36	22	15	39	37
6.02	780	68	27	1	37	12	10	45	59
6.17	898	106	25	4	38	11	13	40	47
6.18	906	79	14	2	49	8	13	51	43
6.33	937	118	32	2	51	28	42	62	22
6.34	942	86	18	3	50	29	23	53	44
6.49	1013	136	23	6	40	11	16	28	61
6.50	1018	51	20	16	61	19	19	56	28
6.66	1097	39	28	7	99	44	23	50	17
6.82	1179	48	17	8	74	20	32	43	19
6.98	1264	45	24	14	64	23	32	39	11
7.14	1351	45	27	12	49	19	21	36	38
7.30	1442	37	22	7	62	19	18	47	30
7.46	1534	32	14	5	52	25	13	36	32
7.62	1629	64	15	2	63	28	43	46	24
7.78	1727	91	22	3	58	20	29	59	23
7.94	1827	115	21	1	70	20	13	46	24
8.10	1929	92	16	1	63	22	32	29	64
8.26	2033	131	30	3	68	16	12	56	21
8.44	2153	79	38	1	60	12	18	49	31
8.60	2262	113	21	1	70	18	17	56	18
8.76	2372	78	27	1	55	22	15	55	30
8.92	2485	137	34	2	79	21	26	51	23

Depth	Age	AM	AC	R3	RS	TP	CE	CH	AX
4.00	11	17	27	17	73	38	1	33	57
4.16	89	18	16	12	52	20	2	95	35
4.32	165	118	19	2	46	12	5	35	55
4.48	238	72	19	0	66	5	4	82	13
4.64	306	113	16	2	32	15	4	98	7
4.80	369	108	10	0	28	4	4	55	22
4.96	426	114	30	2	42	13	20	78	16
5.19	495	143	11	3	50	13	17	51	15

5.35	532	75	14	2	24	13	7	82	10
5.51	561	117	16	2	32	11	21	97	14
5.67	597	72	9	0	73	38	31	70	11
5.83	660	85	16	1	38	16	18	65	40
5.99	758	97	50	1	36	22	15	39	37
6.02	780	68	27	1	37	12	10	45	59
6.17	898	106	25	4	38	11	13	40	47
6.18	906	79	14	2	49	8	13	51	43
6.33	937	118	32	2	51	28	42	62	22
6.34	942	86	18	3	50	29	23	53	44
6.49	1013	136	23	6	40	11	16	28	61
6.50	1018	51	20	16	61	19	19	56	28
6.66	1097	39	28	7	99	44	23	50	17
6.82	1179	48	17	8	74	20	32	43	19
6.98	1264	45	24	14	64	23	32	39	11
7.14	1351	45	27	12	49	19	21	36	38
7.30	1442	37	22	7	62	19	18	47	30
7.46	1534	32	14	5	52	25	13	36	32
7.62	1629	64	15	2	63	28	43	46	24
7.78	1727	91	22	3	58	20	29	59	23
7.94	1827	115	21	1	70	20	13	46	24
8.10	1929	92	16	1	63	22	32	29	64
8.26	2033	131	30	3	68	16	12	56	21
8.44	2153	79	38	1	60	12	18	49	31
8.60	2262	113	21	1	70	18	17	56	18
8.76	2372	78	27	1	55	22	15	55	30
8.92	2485	137	34	2	79	21	26	51	23

Depth	Age	SR	G	R	TU	LG	K	UM	PC
4.00	11	1	2	6	0	0	1	0	0
4.16	89	0	1	0	2	0	0	0	0
4.32	165	0	3	6	2	5	0	0	1
4.48	238	0	4	11	2	4	2	0	0
4.64	306	0	2	6	4	0	0	0	0
4.80	369	0	1	4	3	0	4	2	0
4.96	426	0	1	3	4	1	1	0	1
5.19	495	0	0	2	5	0	2	0	0
5.35	532	0	0	4	58	0	1	0	1
5.51	561	0	0	3	1	0	1	0	1
5.67	597	0	3	3	5	0	3	1	0
5.83	660	0	1	10	7	0	1	1	0
5.99	758	0	5	2	0	0	0	1	0
6.02	780	0	0	7	2	0	2	2	2
6.17	898	0	5	2	4	0	1	1	0
6.18	906	0	2	1	2	0	0	0	0
6.33	937	0	0	1	0	0	0	0	0
6.34	942	1	0	3	3	0	0	0	0
6.49	1013	0	1	5	1	0	0	0	0
6.50	1018	0	0	4	5	0	0	1	0
6.66	1097	1	3	4	1	0	0	1	0
6.82	1179	0	0	4	4	0	0	1	0
6.98	1264	1	0	6	1	0	0	0	0
7.14	1351	0	2	4	5	0	0	2	0
7.30	1442	0	0	3	3	0	1	1	0
7.46	1534	0	0	5	2	0	0	0	0
7.62	1629	1	0	7	1	0	1	0	0
7.78	1727	0	0	1	2	0	0	0	0
7.94	1827	0	0	4	0	0	0	2	0
8.10	1929	0	0	0	4	0	0	0	0
8.26	2033	0	0	2	1	0	0	0	0
8.44	2153	2	1	2	2	0	0	0	0
8.60	2262	0	1	4	0	0	1	0	1
8.76	2372	0	0	2	0	0	0	1	0
8.92	2485	0	0	4	0	0	0	0	0

Depth	Age	BR	UR	CR	CP	L	LA	N	MY
4.00	11	0	0	0	0	0	0	1	1
4.16	89	0	0	1	0	9	0	14	0
4.32	165	0	0	0	1	12	0	2	0
4.48	238	0	0	0	2	1	0	5	1
4.64	306	0	0	0	3	0	0	47	0
4.80	369	0	0	0	3	11	0	5	2
4.96	426	0	0	0	1	1	1	3	1
5.19	495	0	0	0	2	5	0	1	1
5.35	532	0	0	0	1	1	0	0	0
5.51	561	0	0	0	2	0	0	0	1
5.67	597	0	0	0	0	1	0	2	1
5.83	660	0	0	0	0	0	0	4	0
5.99	758	0	0	0	2	0	0	1	0
6.02	780	0	0	0	2	0	0	2	1
6.17	898	0	0	0	1	0	0	2	1
6.18	906	0	0	0	3	0	0	0	1
6.33	937	0	0	0	0	0	0	0	1
6.34	942	0	0	0	2	0	0	2	1
6.49	1013	0	0	0	0	0	0	0	1
6.50	1018	0	0	0	0	0	0	0	0
6.66	1097	2	0	0	0	0	0	0	1
6.82	1179	1	0	0	0	0	0	0	3
6.98	1264	0	0	0	0	0	0	0	0
7.14	1351	0	0	0	0	0	0	0	1
7.30	1442	0	0	0	0	0	0	1	1
7.46	1534	0	0	0	0	0	0	0	1
7.62	1629	0	0	0	0	0	0	0	0
7.78	1727	0	0	0	0	0	0	0	2
7.94	1827	0	0	0	0	0	0	0	1
8.10	1929	0	0	0	0	0	0	0	1
8.26	2033	0	0	0	0	0	0	0	1
8.44	2153	0	0	0	0	0	0	0	1
8.60	2262	0	0	0	0	0	0	0	1

8.76	2372	0	0	0	0	0	0	0	1
8.92	2485	0	0	0	0	0	0	0	0

Depth	Age	UP	PS	PD	PA	PB	PI	Y	EQ
4.00	11	0	2	0	2	0	0	3	0
4.16	89	4	2	0	0	4	0	2	0
4.32	165	4	0	0	1	24	0	3	0
4.48	238	1	0	0	0	6	0	0	0
4.64	306	2	0	0	1	82	0	1	0
4.80	369	2	0	0	0	143	0	3	0
4.96	426	0	0	0	21	37	0	3	0
5.19	495	1	0	0	35	65	0	5	0
5.35	532	1	0	0	15	23	0	11	0
5.51	561	3	0	0	3	4	0	5	0
5.67	597	0	0	0	4	1	0	3	0
5.83	660	1	0	0	3	1	0	2	0
5.99	758	0	0	0	16	4	0	3	0
6.02	780	2	0	0	27	3	0	6	0
6.17	898	2	0	0	17	9	0	1	0
6.18	906	0	0	0	10	12	0	8	1
6.33	937	1	0	0	8	0	0	2	0
6.34	942	0	0	0	10	8	0	3	0
6.49	1013	1	0	0	57	7	0	3	0
6.50	1018	0	0	0	0	0	1	3	0
6.66	1097	0	0	0	0	8	0	4	0
6.82	1179	0	0	0	0	10	0	2	3
6.98	1264	0	0	0	0	2	0	0	0
7.14	1351	1	0	0	0	2	0	2	0
7.30	1442	0	0	0	0	1	0	1	0
7.46	1534	0	0	0	0	1	0	2	0
7.62	1629	0	0	0	0	5	0	3	0
7.78	1727	1	0	0	0	9	0	6	0
7.94	1827	0	0	0	11	7	0	2	0
8.10	1929	1	0	0	22	5	0	5	0
8.26	2033	0	0	0	11	7	0	2	0
8.44	2153	2	0	0	23	291	0	4	0
8.60	2262	0	0	0	15	64	0	1	0
8.76	2372	0	0	0	11	28	0	3	0
8.92	2485	0	0	1	10	12	0	1	0

Depth	Age	DR	TY	PT	LY
4.00	11	0	0	5	565
4.16	89	0	0	4	806
4.32	165	0	0	6	1106
4.48	238	0	0	3	857
4.64	306	0	0	8	936
4.80	369	0	0	1	315
4.96	426	0	0	10	1372
5.19	495	0	0	7	1256
5.35	532	0	0	2	324
5.51	561	0	0	1	352
5.67	597	0	0	1	121
5.83	660	0	1	1	322
5.99	758	0	0	1	738
6.02	780	12	1		431
6.17	898	0	0	6	489
6.18	906	9	0	1	674
6.33	937	1	0	0	86
6.34	942	2	0	1	361
6.49	1013	3	0	0	389
6.50	1018	6	0	2	648
6.66	1097	3	0		488
6.82	1179	0	0	0	315
6.98	1264	0	0	0	247
7.14	1351	2	1	0	385
7.30	1442	3	0	0	245
7.46	1534	6	0	0	356
7.62	1629	4	0	0	216
7.78	1727	15	0	1	381
7.94	1827	3	0	1	105
8.10	1929	2	5	0	125
8.26	2033	3	0	1	156
8.44	2153	7	0	1	153
8.60	2262	2	0	1	108
8.76	2372	1	0	0	123
8.92	2485	1	0	0	95

Depth	Age	HP	H	E	P	AB	HA	LX	CU
9.08	2599	94	32	2	64	27	17	51	28
9.24	2715	89	22	5	62	23	17	54	34
9.40	2833	86	18	5	70	13	24	44	31
9.56	2953	89	19	1	81	41	16	37	22
9.72	3074	75	26	1	86	39	19	34	25
9.88	3196	75	29	5	43	19	9	47	31
10.04	3320	71	24	8	88	34	17	30	28
10.20	3446	92	18	5	96	20	19	48	12
10.36	3572	104	14	7	113	30	16	23	18
10.52	3700	69	22	5	86	20	17	52	31
10.68	3829	93	33	4	69	18	15	29	33
10.84	3960	102	28	2	80	15	11	42	61
11.06	4140	122	11	1	71	7	15	32	62
11.22	4273	81	22	4	91	16	5	21	42
11.38	4407	93	21	5	73	11	9	24	37
11.54	4542	76	20	4	87	9	9	29	46
11.70	4677	80	14	2	54	17	8	39	65
11.86	4814	85	21	6	61	11	21	41	38
12.08	5003	137	11	7	63	19	8	32	35
12.24	5141	122	17	5	63	22	6	25	43
12.40	5281	110	19	6	87	19	14	29	25
12.56	5421	89	23	6	75	16	11	24	46
12.72	5561	109	13	11	98	14	8	17	29
12.88	5703	113	34	4	101	18	11	27	18
13.06	5863	86	31	3	86	20	7	26	30
13.22	6005	138	34	2	84	9	7	11	29
13.39	6157	121	19	7	67	9	7	22	24
13.54	6292	181	28	8	60	12	2	18	48
13.70	6435	96	31	1	68	5	8	7	89
13.86	6580	89	20	3	106	14	7	10	43
14.03	6733	92	21	2	56	7	4	7	89
14.19	6878	64	27	1	75	4	0	10	88
14.35	7024	91	55	14	117	2	1	10	23
14.51	7169	92	36	8	101	4	1	2	55
14.67	7315	98	36	12	101	5	1	13	31
14.83	7461	117	33	5	73	3	1	3	49
15.02	7635	108	44	7	123	11	2	4	29

Depth	Age	AR	AS	CY	S	PU	F	Q1	Q2
9.08	2599	4	0	0	0	0	2	1	36
9.24	2715	2	0	0	5	0	3	1	23
9.40	2833	7	0	0	5	0	4	4	30
9.56	2953	1	0	0	1	0	2	1	32
9.72	3074	5	0	1	1	0	1	4	29
9.88	3196	5	0	1	4	0	0	1	64
10.04	3320	4	2	2	5	0	1	4	19
10.20	3446	2	2	0	2	0	4	2	25
10.36	3572	0	3	1	0	0	1	1	24
10.52	3700	0	0	0	2	0	0	0	32
10.68	3829	2	0	0	6	0	0	0	35
10.84	3960	9	0	0	10	0	1	3	55
11.06	4140	4	0	2	1	0	0	2	29
11.22	4273	4	0	0	2	0	0	2	38
11.38	4407	1	1	1	5	0	1	1	47
11.54	4542	2	0	1	1	0	0	2	50
11.70	4677	4	0	0	7	0	3	2	38
11.86	4814	4	0	0	6	0	0	0	44
12.08	5003	8	1	0	2	0	5	5	26
12.24	5141	0	0	1	3	0	0	4	37
12.40	5281	6	1	0	2	0	0	3	26
12.56	5421	6	0	0	0	0	1	4	43
12.72	5561	1	1	0	3	0	2	9	27
12.88	5703	2	0	0	1	0	0	3	22
13.06	5863	1	0	0	1	0	0	4	41
13.22	6005	0	1	1	1	0	2	3	29
13.39	6157	2	1	0	1	0	2	5	52
13.54	6292	4	1	1	2	0	1	6	51
13.70	6435	4	1	0	1	0	1	1	26
13.86	6580	3	0	0	4	0	3	5	29
14.03	6733	7	0	1	4	0	1	2	38
14.19	6878	11	0	0	3	0	1	2	36
14.35	7024	3	0	0	4	0	1	2	30
14.51	7169	2	0	0	5	0	0	4	25
14.67	7315	1	0	0	3	0	0	1	34
14.83	7461	7	0	1	2	0	1	3	41
15.02	7635	0	0	1	1	0	0	0	17

Depth	Age	AM	AC	R3	RS	TP	CE	CH	AX
9.08	2599	0	3	1	1	0	1	0	0
9.24	2715	0	2	1	0	0	2	1	0
9.40	2833	0	3	1	2	0	1	0	0
9.56	2953	0	2	2	1	0	2	0	0
9.72	3074	0	3	3	1	0	0	1	0
9.88	3196	0	1	1	0	0	1	0	0
10.04	3320	0	1	1	0	0	0	0	0
10.20	3446	0	1	0	0	0	1	1	0
10.36	3572	0	1	0	0	0	0	0	0
10.52	3700	0	0	1	1	0	0	0	0
10.68	3829	0	0	3	2	0	0	1	0
10.84	3960	0	0	1	1	0	2	0	0
11.06	4140	1	2	0	2	0	0	1	0
11.22	4273	0	1	2	3	0	1	1	0
11.38	4407	0	1	1	1	0	1	1	0
11.54	4542	0	4	2	0	0	1	0	0
11.70	4677	0	0	2	0	0	1	0	0
11.86	4814	0	2	4	0	0	1	0	0
12.08	5003	1	1	2	0	0	2	0	0
12.24	5141	0	0	4	1	0	2	0	0
12.40	5281	0	0	3	0	0	0	0	0
12.56	5421	0	0	1	0	0	1	0	0
12.72	5561	0	8	1	1	0	3	0	0
12.88	5703	0	0	0	0	0	0	0	0
13.06	5863	2	1	4	0	0	2	0	0
13.22	6005	0	2	4	1	0	0	0	0
13.39	6157	0	8	1	0	0	2	1	0
13.54	6292	0	6	0	1	0	2	1	0
13.70	6435	0	5	1	1	0	1	1	0
13.86	6580	0	2	2	0	0	1	1	0
14.03	6733	0	4	2	1	0	3	0	0
14.19	6878	0	1	1	1	0	1	0	0
14.35	7024	0	0	1	0	0	0	0	0
14.51	7169	1	1	1	0	0	0	0	0
14.67	7315	1	3	2	0	0	0	0	0
14.83	7461	0	2	1	0	0	0	0	0
15.02	7635	0	0	0	0	0	0	0	0

Depth	Age	SR	G	R	TU	LG	K	UM	PC
9.08	2599	0	0	5	0	0	1	0	0
9.24	2715	0	0	2	2	0	0	0	0
9.40	2833	0	1	4	1	0	1	0	0
9.56	2953	0	0	5	0	0	0	0	0
9.72	3074	0	0	3	2	0	0	0	0
9.88	3196	0	0	2	0	0	2	1	0
10.04	3320	0	0	1	3	0	0	1	0
10.20	3446	0	0	3	2	0	0	0	1
10.36	3572	0	0	5	2	0	0	0	0
10.52	3700	0	1	2	1	0	1	0	0
10.68	3829	1	0	3	1	0	0	2	3
10.84	3960	0	0	8	0	0	1	0	0
11.06	4140	0	0	3	0	0	0	0	0
11.22	4273	0	0	2	2	0	0	0	0
11.38	4407	0	1	5	1	0	0	1	4
11.54	4542	1	2	5	5	1	1	1	0
11.70	4677	0	1	1	4	0	0	1	0
11.86	4814	0	0	3	3	0	1	1	0
12.08	5003	1	1	1	2	0	0	1	1
12.24	5141	0	0	2	2	0	0	1	2
12.40	5281	0	0	6	4	0	0	2	0
12.56	5421	1	1	0	0	0	1	0	0
12.72	5561	0	1	1	2	0	0	0	0
12.88	5703	0	0	4	2	0	0	1	0
13.06	5863	0	0	2	4	1	1	1	0
13.22	6005	1	1	6	4	0	1	0	0
13.39	6157	1	0	7	1	0	3	0	0
13.54	6292	0	0	4	3	0	1	1	0
13.70	6435	0	0	0	5	1	1	0	0
13.86	6580	2	0	1	1	0	0	0	0
14.03	6733	0	0	4	1	0	1	0	0
14.19	6878	0	0	1	3	0	1	0	0
14.35	7024	0	0	2	1	0	0	0	0
14.51	7169	1	0	3	2	0	0	0	3
14.67	7315	0	1	1	4	0	0	0	0
14.83	7461	1	0	3	4	0	1	1	0
15.02	7635	0	0	0	1	0	0	1	2

Depth	Age	BR	UR	CR	CP	L	LA	N	MY
9.08	2599	2	0	0	1	0	0	0	0
9.24	2715	0	0	0	3	0	0	0	0
9.40	2833	0	0	0	0	0	0	2	0
9.56	2953	0	0	0	3	0	0	0	0
9.72	3074	0	0	0	2	0	0	1	0
9.88	3196	0	0	0	0	0	0	1	0
10.04	3320	0	0	0	0	0	0	0	2
10.20	3446	0	0	0	0	0	0	0	2
10.36	3572	0	0	0	0	0	0	0	0
10.52	3700	0	0	0	0	0	0	1	0
10.68	3829	0	0	0	0	0	0	0	1
10.84	3960	0	0	0	0	0	0	0	0
11.06	4140	0	0	0	1	0	0	0	0
11.22	4273	0	0	0	0	0	0	1	0
11.38	4407	0	0	0	3	0	0	1	0
11.54	4542	0	0	0	0	0	0	0	1
11.70	4677	0	0	0	1	0	0	1	0
11.86	4814	0	0	0	0	0	0	0	1
12.08	5003	0	0	0	0	0	0	0	0
12.24	5141	0	0	0	1	0	0	3	1
12.40	5281	0	0	0	0	0	0	0	0
12.56	5421	0	0	0	0	0	0	0	1
12.72	5561	0	0	0	0	0	0	0	0
12.88	5703	0	0	0	1	0	0	0	0
13.06	5863	0	0	0	0	0	0	0	0
13.22	6005	0	0	0	2	0	0	0	1
13.39	6157	0	0	0	1	0	0	0	1
13.54	6292	0	0	0	1	0	0	1	1
13.70	6435	0	0	0	2	0	0	0	0
13.86	6580	0	0	0	2	0	0	0	0
14.03	6733	0	0	0	2	0	0	1	0
14.19	6878	0	0	0	0	0	0	0	1
14.35	7024	0	0	0	0	0	0	0	0
14.51	7169	0	0	0	0	0	0	1	1
14.67	7315	0	0	0	0	0	0	0	0
14.83	7461	0	0	0	0	0	0	0	0
15.02	7635	0	0	0	0	0	0	0	0

Depth	Age	UP	PS	PD	PA	PB	PI	Y	EQ
9.08	2599	0	0	0	4	19	0	3	0
9.24	2715	2	0	2	3	22	0	6	0
9.40	2833	2	0	10	0	7	0	1	0
9.56	2953	0	0	4	0	17	0	1	0
9.72	3074	0	0	3	1	14	0	0	0
9.88	3196	0	0	0	0	15	0	0	0
10.04	3320	0	0	0	0	3	0	1	0
10.20	3446	0	0	0	0	9	0	1	0
10.36	3572	0	0	0	0	9	0	0	0
10.52	3700	1	0	0	3	8	0	0	0
10.68	3829	0	0	0	0	12	0	2	0
10.84	3960	0	0	0	7	21	0	3	0
11.06	4140	0	0	0	5	38	0	2	0
11.22	4273	0	0	0	5	24	0	0	0
11.38	4407	1	0	0	0	2	0	2	0
11.54	4542	1	0	0	6	11	0	3	0
11.70	4677	1	0	0	1	8	0	0	0
11.86	4814	0	0	0	1	18	0	1	0
12.08	5003	0	0	0	5	3	0	1	0
12.24	5141	0	0	0	7	5	0	1	0
12.40	5281	0	0	0	5	11	0	2	0
12.56	5421	2	0	0	5	8	0	5	0
12.72	5561	0	0	0	3	6	0	6	0
12.88	5703	0	0	0	1	1	0	1	0
13.06	5863	1	0	0	2	2	0	0	0
13.22	6005	0	0	0	1	3	0	2	0
13.39	6157	0	0	0	1	1	0	1	0
13.54	6292	0	0	0	3	3	0	5	0
13.70	6435	0	0	0	0	0	0	4	0
13.86	6580	1	0	0	1	2	0	6	0
14.03	6733	0	0	0	0	4	0	2	0
14.19	6878	0	0	0	0	1	0	3	0
14.35	7024	0	0	0	0	0	0	0	0
14.51	7169	0	0	0	0	0	0	2	0
14.67	7315	0	0	0	0	5	0	2	0
14.83	7461	0	0	0	0	2	0	3	0
15.02	7635	0	0	0	0	0	0	0	0

Depth	Age	DR	TY	PT	LY
9.08	2599	8	1	0	88
9.24	2715	3	1	0	88
9.40	2833	1	0	0	110
9.56	2953	1	0	0	170
9.72	3074	0	1	0	144
9.88	3196	1	0	0	121
10.04	3320	2	0	0	232
10.20	3446	0	0	0	153
10.36	3572	5	0	0	134
10.52	3700	10	0	0	132
10.68	3829	18	0	0	182
10.84	3960	11	0	0	186
11.06	4140	24	0	1	71
11.22	4273	14	0	1	108
11.38	4407	0	0	0	284
11.54	4542	0	0	0	180
11.70	4677	0	0	0	147
11.86	4814	0	0	0	72
12.08	5003	0	0	1	107
12.24	5141	0	0	0	104
12.40	5281	0	0	0	102
12.56	5421	0	0	0	90
12.72	5561	0	0	0	95
12.88	5703	0	0	0	88
13.06	5863	0	0	0	50
13.22	6005	0	0	0	97
13.39	6157	0	0	0	81
13.54	6292	0	0	1	89
13.70	6435	0	0	0	103
13.86	6580	0	0	0	47
14.03	6733	0	0	2	68
14.19	6878	0	0	0	154
14.35	7024	0	0	0	95
14.51	7169	0	0	1	124
14.67	7315	0	0	0	82
14.83	7461	0	0	1	93
15.02	7635	0	0	0	107

Depth	Age	HP	H	E	P	AB	HA	LX	CU
15.18	7782	112	14	11	91	0	2	5	65
15.34	7928	122	8	7	74	7	2	1	67

Depth	Age	AR	AS	CY	S	PU	F	Q1	Q2
15.18	7782	8	0	0	2	0	2	0	36
15.34	7928	10	0	2	3	1	0	2	54

Depth	Age	AM	AC	R3	RS	TP	CE	CH	AX
15.18	7782	1	0	2	0	0	0	0	0
15.34	7928	1	0	4	1	0	0	0	0

Depth	Age	SR	G	R	TU	LG	K	UM	PC
15.18	7782	0	0	4	1	0	0	0	0
15.34	7928	0	3	0	2	0	0	0	0

Depth	Age	BR	UR	CR	CP	L	LA	N	MY
15.18	7782	0	0	0	0	0	0	0	4
15.34	7928	0	0	0	0	0	0	0	0

Depth	Age	UP	PS	PD	PA	PB	PI	Y	EQ
15.18	7782	0	0	0	0	0	0	0	0
15.34	7928	0	0	0	0	2	0	4	0

Depth	Age	DR	TY	PT	LY
15.18	7782	0	0	0	68
15.34	7928	0	0	0	178